REMARKS

Claims 1 and 3-29, as amended, are pending in this application for the Examiner's review and consideration. Claim 1 has been amended to explicitly specify that step (b) is performed after step (a), and step (c) is performed after step (b), support for which can be found in the specification, e.g., paragraphs [0012] and [0113] of the published application as well as in Applicants' prior submissions. As no new matter has been introduced by this change, it should be entered at this time to reduce the issues for appeal by clarifying the scope of the claims.

Claim Rejections – 35 USC § 102

Claims 1, 3-7, 9, 10, 15-21, 23, 24, 29-31 and 36 have been rejected under 35 U.S.C. 102(b) as allegedly being anticipated by U.S. Patent Application No. 2003/0208152 to Avrahami et al. (referred hereafter as "Avrahami"). The Office Action alleges that regarding claims 1 and 16, Avrahami discloses a method of delivering an oligonucleotide or polynucleotide via the following: generating at least one micro-channel in the skin of a subject (Paragraph 17) and applying to the skin a pharmaceutical composition of an acceptable carrier (conductive substance – Paragraph 32) with an active ingredient (Paragraph 33) of an oligonucleotide or polynucleotide (Paragraph 255). The Office Action further alleges that Avrahami also discloses two different subsets for generating the micro-channels (Paragraphs 55-58).

Applicant respectfully disagrees. Avrahami discloses devices and methods for enhancing transdermal movement of a substance. The methods of Avrahami comprise a step of generating at least one micro-channel in the stratum corneum to enable or augment transdermal movement of the substance (see, for example, paragraphs [0017], [0036], [0037], [0112], [0137], [0167] of Avrahami). The substance according to Avrahami is actively or passively delivered to the skin following ablation of the skin (see, for example, paragraphs [0037], [0137], and [0167] of Avrahami). Devices and methods for actively delivering the substance are disclosed in Avrahami: a pressure generating unit used to propel the active substance by gas, an ultrasonic transducer, or iontophoresis (see, for example, paragraphs [0041] and [0042] of Avrahami). Thus, Avrahami discloses devices and methods for forming micro-channels by ablating the stratum corneum in order to increase conductance of the substances therethrough (see, for example, paragraph [0020] of Avrahami). In all embodiments, Avrahami generates micro-channels prior to application of an active substance (see, e.g., paragraphs [0037] and [0042]).

The Office Action asserts that iontophoresis and electroporation, while forming smaller channels, still form channels that may be measured on the micro scale and that Avrahami discloses iontophoresis being used in conjunction with ablation. Applicant wishes to clarify that although iontophoresis and electroporation involve electric fields, neither of these methods form channels on a micro scale. In particular, iontophoresis acts primarily on the substance, propelling it through the skin by repulsive electromotive force and causing skin structural changes only as a secondary effect. Moreover, as shown in the enclosed publication by Prausnitz et al. (Proc. Natl. Acad. Sci. U.S.A., 90: 10504-10508, 1993), electroporation forms transient aqueous pores in the lipid bilayers of the stratum corneum by application of short electric pulses. The transient pores formed during electroporation, usually of a radius of several nanometers, tend to close within 10^{-3} seconds to minutes (see, for example, the enclosed publication by Freeman et al., Biophys. J. 67: 42-56, 1994, particularly Figs. 7 and 11). Thus, neither iontophoresis nor electroporation is associated with ablation/removal/destruction of the stratum corneum. In contrast, the micro-channel generation of the present invention takes place as a result of ablation of the stratum corneum by electrical energy (see, for example, paragraphs [0024] to [0027], [0100], and [0101] of the published application). The micro-channels generated have a diameter of tens to hundreds of microns (see, for example, paragraphs [0103], [0123], and [0170] of the published application). Thus, iontophoresis and electroporation are distinct methods that are recognized by skilled artisans as being distinct from each other. They also are entirely different from the presently claimed method which involves generation of micro-channels.

The Office Action also asserts that Avrahami discloses two different subsets for generating the micro-channels. Indeed, Avrahami discloses a substance delivery unit adapted to drive a first subset of electrodes to apply during a first time period a current capable of ablating stratum corneum in the vicinity of the first subset of electrodes and to drive a second subset of electrodes to apply during a second time period a current capable of ablating stratum corneum in vicinity of the second subset of electrodes (see paragraphs [0055] to [0057] of Avrahami). Avrahami explicitly discloses that the current applied by the first and second subsets of electrodes is responsive to a desired rate of delivery of the substance during a first time period and a second time period, respectively (see paragraphs [0052] to [0054] of Avrahami). In other words, Avrahami unambiguously teaches methods of transdermal delivery wherein micro-

channel generation is characteristically performed prior to the delivery of the substance. Avrahami neither discloses nor suggests a method which comprises the steps of generating micro-channels both before and after application of an oligonucleotide or polynucleotide (e.g., present claim 1) or only after such application (e.g., present claim 16).

In contrast, the present invention discloses that generating micro-channels in an area of the skin before application of a pharmaceutical composition comprising an oligonucleotide or polynucleotide to that area of the skin and also after such application enhances the transdermal delivery of the oligonucleotide or polynucleotide if compared to the delivery obtained by generating micro-channels only before application of the pharmaceutical composition (see paragraphs [0012] and [0113] of the published application). In order to further distinguish the present invention from Avrahami, claim 1 has been amended to explicitly recite that step (b) is performed after step (a), and step (c) is performed after step (b). Claim 1 now is clearly directed to a method for intradermal or transdermal delivery of an oligonucleotide or polynucleotide wherein a first plurality of micro-channels is initially generated in an area of the skin of a subject; thereafter the pharmaceutical composition is applied to the area of the skin of the subject where the first plurality of micro-channels are present; and after that a second plurality of micro-channels are generated in the area where the composition is applied to facilitate the delivery of the oligonucleotide or polynucleotide of the pharmaceutical composition. It should be noted that claim 16 as previously presented already includes this inherent order because it recites that the micro-channels are generated after the application of the composition.

Thus, both claim 1 as amended and claim 16 as previously presented recite generating micro-channels after the application of the composition, and hence are not anticipated by Avrahami which only discloses generating micro-channels prior to the application of the composition. As claims 3-7, 9, 10, and 15 depend from claim 1 and recite additional features, and as claims 17-21, 23, 24, and 29 depend from claim 16 and recite additional features, these claims are also not anticipated by Avrahami. Accordingly, the rejection of claims 1 and 16, and of the claims dependent therefrom under 35 U.S.C. 102(b) over Avrahami should be withdrawn.

Claim Rejections – 35 USC § 103

Claims 8 and 22 have been rejected under 35 U.S.C. 103(a) as allegedly being unpatentable over Avrahami as applied to claim 1, and further in view of U.S. Patent No.

6,429,200 to Monahan et al. (referred hereafter as "Monahan"). The Office Action asserts that while Avrahami substantially discloses the apparatus as claimed, it does not disclose additives to the active agent such as lipids, polycations or nuclease inhibitors. The Office Action further asserts that Monahan discloses adding polycations to polynucleotides and reverse micelles in order to compact the polynucleotides. The Office Action thus concludes that it would have been obvious to one of ordinary skill in the art at the time the invention was made to modify the delivery device/method of Avrahami to utilize polycations and reverse micelles as taught by Monahan to compact the polynucleotides for gene delivery purposes.

Applicant respectfully disagrees. As indicated above, Avrahami does not disclose or suggest a method for intradermal or transdermal delivery of an oligonucleotide or polynucleotide by generating micro-channels in the skin after application of a composition that contains an oligonucleotide or polynucleotide, as presently claimed.

Monahan does not remedy the deficiencies of Avrahami. Monahan discloses a process for delivering a complex to a cell comprising inserting a nucleic acid into a reverse micelle (col. 5, lines 55-63 of Monahan). According to Monahan, compounds can be added to the nucleic acid/micelle mixture. Among the compounds, polymers such as polyions (polycations, polyamines, and polyanions) are listed (see, e.g., col. 5, line 67 through col. 6, line 6 of Monahan). Monahan does not disclose or suggest generating micro-channels after the application of the composition. Thus, even if one of ordinary skill in the art combines Avrahami and Monahan, he would not obtain the methods of intradermal or transdermal delivery of oligonucleotide or polynuleotide as recited in claims 8 and 22, which add further features to claims 1 and 16, respectively. Therefore, the rejection of these claims should be withdrawn.

Claims 10-14, 24-28 and 31-35 have been rejected under 35 U.S.C. 103(a) as allegedly being unpatentable over Avrahami. The Office Action asserts that regarding claims 10, 24, and 31, it would have been obvious to one of ordinary skill in the art at the time the invention was made to generate micro-channels of uniform shape and dimension so as to homogenously deliver the active agent which is notoriously well known within the art as being more desirable than uneven delivery absent any other considerations. Regarding claims 11-14, 25-28, and 32-35, the Office Action asserts that it would have been obvious matter of design choice to a person of ordinary skill in the art to determine and assign diameters and lengths to the electrodes because Applicant has not disclosed that such a limitation provides an unexpected advantage.

Applicant respectfully disagrees. As explained herein, Avrahami does not disclose or suggest the methods recited and claimed in claims 1 and 16. Therefore, claims 1 and 16 are patentable over Avrahami. As claims 10-14 and 24-28 depend from claims 1 and 16, respectively, and include additional features, these claims are patentable over Avrahami, and therefore the rejection of these claims should be withdrawn. The rejections of claims 31-35 should be withdrawn as these claims have been cancelled.

Claims 15, 29, and 36 have been rejected as allegedly being unpatentable over Avrahami as applied to claim 9, and further in view of U.S. Patent Application No. 2005/0287217 (referred hereafter as "Levin") and U.S. Patent No. 6,148,232 (referred hereafter as "Avrahami '232").

As indicated above, Avrahami does not disclose or suggest the methods recited in claims 1 and 16. Levin and Avrahami '232 do not remedy the deficiencies of Avrahami. In particular, Avrahami '232 discloses a device for ablating the stratum corneum epidermidis of a subject, including a plurality of electrodes, which are applied to the subject's skin at respective points. A power source applies electrical energy between two or more of the plurality of electrodes, in order to cause ablation of the stratum corneum primarily in an area intermediate the respective points (see, e.g., abstract of Avrahami '232). According to Avrahami '232, micro-channels are generated in the stratum corneum to enable or augment transdermal movement of a substance (see, e.g., col. 2, lines 59-67 of Avrahami '232), namely micro-channels are generated before application of a drug (see, e.g., col. 6, lines 29-33 of Avrahami '232).

Levin discloses a method for intradermal or transdermal delivery of water soluble, poorly soluble, or insoluble cosmetic agents comprising: (i) generating at least one micro-channel in a region of skin of a subject suffering from a skin condition; and (ii) topically applying a cosmetic or dermatological composition comprising a dermatologically effective amount of at least one water-soluble, poorly water-soluble, or water-insoluble cosmetic agent and a cosmetically or dermatologically acceptable carrier to the region of the skin in which the micro-channels are present so as to improve the skin condition of said subject (see, e.g., paragraphs [0030] to [0032] of Levin). Thus, according to Levin, the micro-channels are also generated before application of a dermatological or cosmetic composition.

Therefore, even if one of ordinary skill in the art combines Avrahami, Levin, and Avrahami '232, he would not obtain the methods as recited and claimed in claims 1 and 16, and therefore claims 1 and 16 are patentable over Avrahami in view of Levin and Avrahami '232.

Applicant respectfully submits that the teachings of generating micro-channels prior to administration of a composition do not render unpatentable claims directed to generating micro-channels after application of the composition. Also, as claims 15 and 29 depend from claims 1 and 16, respectively, and include additional features, claims 15 and 29 are also patentable over Avrahami in view of Levin and Avrahami '232. Accordingly, the rejection of these claims should be withdrawn. The rejections of claim 36 should be withdrawn as it has been cancelled.

In view of the above, it is respectfully submitted that all current rejections have been overcome and should be withdrawn. Accordingly, the entire application is believed to be in condition for allowance, early notice of which would be appreciated. Should the Examiner not agree, then a personal or telephonic interview is respectfully requested to discuss any remaining issues and expedite the eventual allowance of this application.

Respectfully submitted,

Date: 11/30/10

Allan A. Fanucci (Reg. No. 30,256)

WINSTON & STRAWN LLP
CUSTOMER NO. 28765
(212) 294-3311

Proc. Natl. Acad. Sci. USA
Vol. 90, pp. 10504–10508, November 1993
Medical Sciences

Electroporation of mammalian skin: A mechanism to enhance transdermal drug delivery

(stratum corneum/lipid bilayer/electropermeabilization/tissue/iontophoresis)

MARK R. PRAUSNITZ*, VANU G. BOSE†, ROBERT LANGER*‡§, AND JAMES C. WEAVER‡§

Departments of *Chemical Engineering and of †Electrical Engineering and Computer Science, and ‡Harvard–MIT Division of Health Sciences and Technology, Massachusetts Institute of Technology, Cambridge, MA 02139

Communicated by Andreas Acrivos, August 10, 1993 (received for review May 19, 1993)

ABSTRACT **Mammalian skin owes its remarkable barrier function to its outermost and dead layer, the stratum corneum. Transdermal transport through this region occurs predominantly through intercellular lipids, organized largely in bilayers. Electroporation is the creation of aqueous pores in lipid bilayers by the application of a short (microseconds to milliseconds) electric pulse. Our measurements suggest that electroporation occurs in the intercellular lipid bilayers of the stratum corneum by a mechanism involving transient structural changes. Flux increases up to 4 orders of magnitude were observed with human skin *in vitro* for three polar molecules having charges between −1 and −4 and molecular weights up to slightly more than 1000. Similar flux increases were observed *in vivo* with animal skin. These results may have significance for drug delivery and other medical applications.**

Transdermal drug delivery offers a number of potential advantages over conventional methods, such as pills and injections: (i) no degradation due to stomach, intestine, or first pass of the liver, (*ii*) probable improved patient compliance because of a user-friendly method, and (*iii*) potential for steady or time-varying controlled delivery (1–4). Nevertheless, very few drugs can be administered transdermally at therapeutic levels, due to the low permeability and lipophilic nature of human skin. As a result, fewer than 10 drugs are now clinically administered transdermally. However, the market for these drugs exceeds one billion dollars in the United States alone, indicating the importance of this delivery method. Therefore, significant enhancement of transdermal drug delivery has the potential for major impact on medicine.

A number of approaches have been taken to increase transdermal transport (2–4). Most common is the addition of chemical enhancers, compounds which are believed to increase the partitioning of drugs into the skin. Another approach is chemical modification of a drug into a "prodrug," which penetrates the skin well but is subsequently converted by epidermal enzymes into the original pharmacologically active drug. Application of ultrasound has been used as well to increase transdermal flux and to reduce transport lag times. Yet another approach is iontophoresis, the movement of drugs across the skin by an electric field. Mechanistically similar to electrophoresis, iontophoresis is believed to act primarily by moving charged species across the skin by an electrical force.

The barrier properties of skin are attributed primarily to the stratum corneum, the skin's outer layer. The stratum corneum is a dead tissue composed of flattened cells filled with crosslinked keratin and an extracellular matrix made up of lipids arranged largely in bilayers (5, 6). Unlike the unilamellar phospholipid bilayers of cell membranes, these multilamellar, extracellular bilayers contain no phospholipids, being composed primarily of ceramides, cholesterol, and fatty acids (1–3). Intercellular pathways are generally the most important routes for transdermal transport (1–3). Therefore, permeabilization of the lipid bilayers filling these intercellular pathways would be expected to increase transdermal transport.

Electroporation is a method of reversibly permeabilizing lipid bilayers, involving the creation of transient aqueous pores by the application of an electric pulse (7, 8). Dramatically reduced electrical resistance and extensive transport of molecules, including macromolecules, are generally associated with electroporation of lipid bilayers, including membranes of artificial planar and spherical systems, as well as those of living cells. Electric field exposures causing electroporation typically generate transmembrane potentials of $\approx$1 V and last 10 μsec to 10 msec. Electroporation of isolated single cells is well established, but electroporation of cells that are part of an intact tissue has received little attention (9–12). To our knowledge, electroporation of multilamellar or non-phospholipid systems has not been previously demonstrated.

In this study, we examine the possibility of electroporating the multilamellar, non-phospholipid, intercellular lipid bilayers of the stratum corneum as a mechanism to enhance transdermal drug delivery. Although both electroporation and iontophoresis involve electric fields, the two approaches are fundamentally different. While iontophoresis acts primarily on the drug, involving skin structural changes as a secondary effect (2, 3), electroporation is expected to act directly on the skin, making transient changes in tissue permeability. Because electroporation of cells has been shown to increase transmembrane fluxes dramatically and reversibly, electroporation of skin could make possible the transdermal delivery of many more drugs at therapeutic levels.

MATERIALS AND METHODS

Materials. Phosphate-buffered saline (PBS) was prepared containing 138 mM NaCl, 8.1 mM Na_2HPO_4, 2.7 mM KCl, and 1.1 mM KH_2PO_4 (Mallinckrodt) and was adjusted to pH 7.4 by adding NaOH or HCl (Mallinckrodt). Calcein was obtained from Sigma and Molecular Probes. Lucifer yellow and erythrosin-5-iodoacetamide were obtained from Molecular Probes. To make the sulfur-alkylated erythrosin derivative, erythrosin-5-iodoacetamide was incubated with excess 6-mercapto-1-hexanol in PBS at 25°C for >12 hr.

Skin Preparation. By use of established methods for skin sample preparation, full-thickness excised cadaver skin was obtained within 48 hr after death and stored at 4°C and 95% humidity for up to 1 week (2, 3). Full-thickness samples were prepared by gently scraping off subcutaneous fat. Epidermis samples were heat separated by submerging full-thickness

The publication costs of this article were defrayed in part by page charge payment. This article must therefore be hereby marked "*advertisement*" in accordance with 18 U.S.C. §1734 solely to indicate this fact.

§To whom reprint requests should be addressed.

skin in 60°C water for 2 min and gently removing the epidermis (13). All samples were stored at 4°C and 95% humidity for <3 weeks. Tissue was obtained from four sources (three local hospitals and the National Disease Research Interchange) to minimize any artifacts of tissue acquisition. Tissue was generally from the abdomen, removed just lateral to the midline, although tissue from the breast, back, and thigh have been used as well.

Because the primary barrier to transport is the stratum corneum (the upper 10–20 μm of the epidermis), the use of epidermis rather than full-thickness skin is a well-established model for transdermal drug delivery (2, 3). In the literature, transdermal drug delivery is commonly understood to mean transport of drugs across the skin (not just the dermis) (1–4). When systemic delivery is desired, a drug must traverse the stratum corneum, the viable epidermis, and some fraction of the dermis before entering blood vessels of the systemic circulation. Since capillaries exist near the dermal/epidermal junction, drugs can enter the systemic circulation without crossing the whole dermis (1–3). Thus, transport across full-thickness skin misrepresents the actual transport pathway. For these reasons, following established practice (2, 3), we have performed the majority of our studies with human epidermis and have established agreement with select results from full-thickness human skin.

***In Vitro* Methods.** Prepared skin samples were loaded into side-by-side permeation chambers (14), exposed to well-stirred PBS, and allowed to hydrate fully (12–18 hr, 4°C). The temperature was raised to 37°C and fresh PBS was added, with 1 mM fluorescent compound (calcein, Lucifer yellow, or erythrosin derivative) on the outer, stratum corneum side. After a steady-state flux was established (within a few hours), electric pulsing was applied with Ag/AgCl electrodes (≈2 cm from skin) (In Vivo Metrics, Healdsburg, CA). An exponential-decay pulse (τ = 1.0–1.3 msec; Gene-Pulser; Bio-Rad) was applied every 5 sec for 1 hr, with the negative electrode on the stratum corneum side ("forward" pulsing), except for "reverse" pulsing, where the positive electrode was on the stratum corneum side. Iontophoresis (continuous dc voltage) was also used for 1 hr, with the negative electrode on the stratum corneum side. The receptor compartment was sampled periodically by emptying its contents and replacing it with fresh PBS. Analysis by calibrated spectrofluorimetry (Fluorolog-2, model F112AI; Spex Industries, Metuchen, NJ) allowed measurement of fluorescent compound concentrations in the receptor compartment and, thereby, calculation of transdermal fluxes.

Reported voltages are transdermal values, determined at >1 μsec after the onset of the pulse. During a pulse, the apparent resistance of the chamber, without skin (but including electrodes, saline, and interfacial resistances), was 480 Ω, independent of the pulse voltage. The apparent resistance of the chamber with skin varied from 900 Ω during lower-voltage pulses (≈50 V across skin) to 600 Ω during higher-voltage pulses (≈500 V across skin), meaning that only 20–50% of the applied voltage appeared across the skin. Transdermal voltages were determined by calculating the ratio of the apparent skin resistance to the apparent total chamber (with skin) resistance. This ratio is equal to the ratio of the transdermal voltage to the voltage across the whole chamber (with skin). By application of a voltage pulse and measurement of the resulting current, apparent resistances were calculated by dividing the applied voltage by the measured current.

Post-pulse skin electrical characterization was performed with a four-electrode impedance-measurement system. A current step (2 μA/cm^2) was applied and the resulting transdermal voltage was measured. By using a Fourier transform, skin impedance was calculated over a range of frequencies (1–1000 Hz) by dividing the measured transdermal voltage by the applied current.

***In Vivo* Methods.** For *in vivo* studies, reservoirs (≈4 ml, 2.8 cm^2) with Ag/AgCl electrodes (≈1 cm from skin) were attached to gently pinched skin from the caudal dorsal region of anesthetized (ketamine, 75 mg/kg, and xylazine, 10 mg/kg, with additional one-third doses given every 30–45 min) CD hairless rats (Charles River Breeding Laboratories) (12); animal care was in accordance with institutional guidelines. Hairless rodents are commonly used as *in vivo* models for transdermal studies (2, 3). Both reservoirs were filled with PBS; the negative electrode side contained 10 mM calcein. Pulses were applied as described above for 1 hr.

Plasma calcein concentration measurements were made 30–60 min after pulsing. Blood samples were taken from the lateral tail vein, transferred into a serum separator tube (Microtainer, Becton Dickinson), and spun at 1000 × *g* for 5 min to isolate the plasma for analysis by calibrated spectrofluorimetry. The appropriate volume of distribution of calcein within the rat was determined by measuring plasma concentrations over time following intravenous and subcutaneous injections of known amounts of calcein. Maximum plasma concentrations were measured 30–60 min after injection, suggesting that significant metabolism or elimination did not occur over that period (15, 16). The volume of distribution determined from these measurements was 20% of total rat volume (17), which is equal to the volume of the extracellular aqueous compartment (18). Given the very hydrophilic nature of calcein (19), distribution throughout all extracellular aqueous regions is a reasonable assumption.

RESULTS AND DISCUSSION

To determine whether electroporation of the stratum corneum was possible, we subjected human cadaver epidermis under physiological conditions to electric pulses which cause electroporation in other systems. Quantitative measurements of transdermal molecular flux, supported by electrical measurements, are consistent with three unique characteristics of electroporation (7, 8): (*i*) large increases in molecular flux and ionic conductance, (*ii*) reversibility over a range of voltages, and (*iii*) changes in barrier membrane structure.

First, transdermal fluxes of calcein (623 Da, −4 charge), a moderate-sized, highly polar molecule which does not normally cross skin in detectable quantities, were measured during application of low-duty-cycle electric-field pulses. Fig. 1 shows average transdermal fluxes of calcein before, during, and after pulsing at representative voltages. Fluxes before pulsing were below the detection limit (imposed by background fluorescence), whereas fluxes during pulsing were up to 4 orders of magnitude above this limit. Fig. 2 shows that flux increased nonlinearly with increasing pulse voltage, where flux increased strongly with increasing voltage below ≈100 V and increased weakly with increasing voltage at higher voltages. Supporting electrical measurements also showed increases in skin conductance of 1–3 orders of magnitude. Electrical changes were evident during the pulse and immediately (≥10 msec) after. This is consistent with changes caused by electroporation, the onset of which is believed to occur on the microsecond scale (20–22).

Second, reversibility was assessed. Following electrical pulsing for 1 hr, transdermal fluxes generally decreased by about 90% within 30 min and by >99% within 1 or 2 hr (Fig. 1), indicating significant reversibility. Electrical conductance measurements also showed recovery, either complete or to within a factor of 3 of pre-pulse values. However, elevated post-pulsing fluxes could be caused not only by irreversible alterations of skin structure but also by the efflux of calcein "loaded" into the skin during high fluxes during pulsing (23, 24).

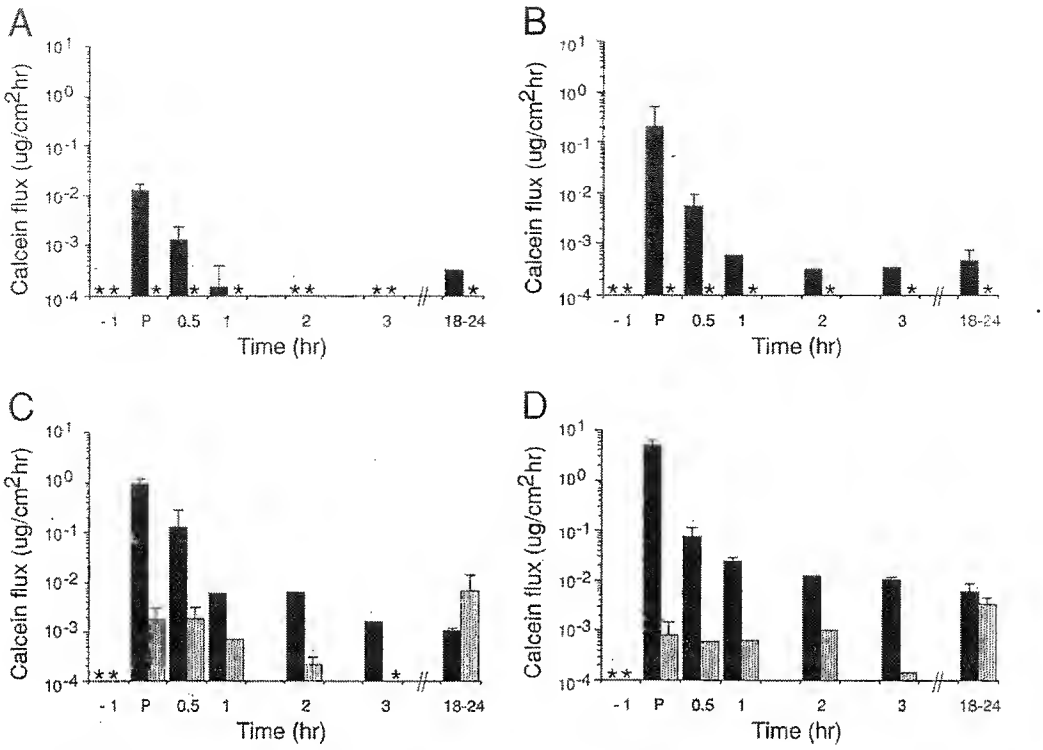

FIG. 1. Transdermal fluxes of calcein (623 Da, −4 charge) before, during, and after "forward" pulsing (solid bars) or "reverse" pulsing (stippled bars) at 55 V (*A*), 90 V (*B*), 165 V (*C*), and 300 V (*D*). Flux increases up to 4 orders of magnitude are observed under "forward" pulsing conditions (see text). These increases are at least partially reversible. "Reverse" pulsing facilitates independent assessment of changes in skin permeability due to electroporation (see text), suggesting that skin electroporation may be fully reversible below ≈100 V, under the conditions used. Fluxes are shown 1 hr before pulsing, during pulsing (P), and at times after pulsing. Pulsing was performed for 1 hr (see text). Elevated fluxes at 18–24 hr could be caused by skin deterioration. Each point represents the average of three to seven skin samples, from two to four different subjects. Standard deviation bars are shown. Asterisk indicates a flux below the detection limit, of order 10^{-4} μg/(cm²hr).

The results of an additional, and possibly better, test of reversibility are also shown in Fig. 1: skin was pulsed with the electrode polarity reversed, leaving the transmembrane voltage magnitude during pulsing the same. However, the electrophoresis associated with the pulse should move calcein away from the skin under these conditions, markedly reducing transdermal transport during pulsing. By measuring fluxes ≈1 hr after reverse-pulsing, long-lived changes in skin permeability can be assessed independently, as summarized in Fig. 2. These data suggest that pulses at or below ≈100 V cause no detectable long-lived changes in skin permeability. However, higher voltage pulses appear to cause lasting changes; these changes do not go away, even after 18–24 hr. Fig. 2 also suggests that a transition region may exist at ≈100 V, below which flux increases as a strong function of voltage and flux increases are reversible, and above which flux increases only weakly with voltage and effects are only partially reversible. The exact mechanism underlying this transition is unclear.

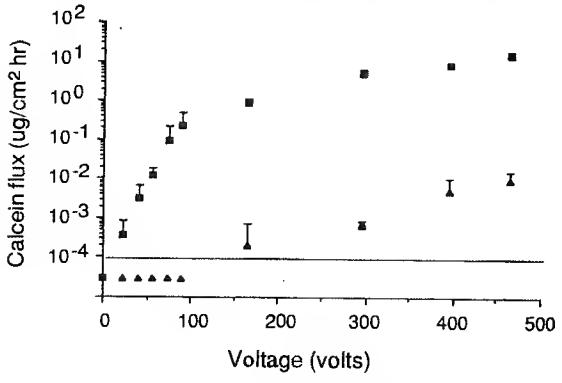

FIG. 2. Transdermal fluxes of calcein due to exposure of human skin to different electrical conditions. Calcein flux during application of forward-polarity pulses (■) and ≈1 hr after pulsing in the reverse direction (see text) (▲). This figure suggests that a transition point may exist at ≈100 V, below which flux increases as a strong function of voltage and flux increases are reversible, and above which flux increases only weakly with voltage and effects are only partially reversible. Each point represents the average of three to seven skin samples, from two to four different subjects. Standard deviation bars are shown. Fluxes below the calcein flux detection limit are indicated below the dashed line.

Third, changes in skin structure cannot be expected to be revealed by microscopy, for reasons discussed below. However, demonstrating that increased fluxes caused by pulsing cannot be explained by electrophoresis alone suggests that changes in skin structure are necessary to explain our results. We therefore compared fluxes caused by low-duty-cycle high-voltage pulsing to fluxes caused by the continuous low-voltage dc current which would provide the same total electrophoretic component if no changes in skin structure occurred. For example, if the skin were unaltered (i.e., same conductance), then continuous application of 0.1 V would transfer the same amount of charge across the skin as the pulsed application of 500 V for 1 msec every 5 sec, making these conditions electrophoretically "equivalent." As seen in Fig. 3, application of continuous voltages caused fluxes 3 orders of magnitude smaller than pulsing under "equivalent" conditions, suggesting that skin structural changes are needed to explain these results.

To assess the occurrence and reversibility of electroporation, we believe that characterization of flux changes, along with companion electrical measurements, is the best approach, since these measures are universally accepted in the

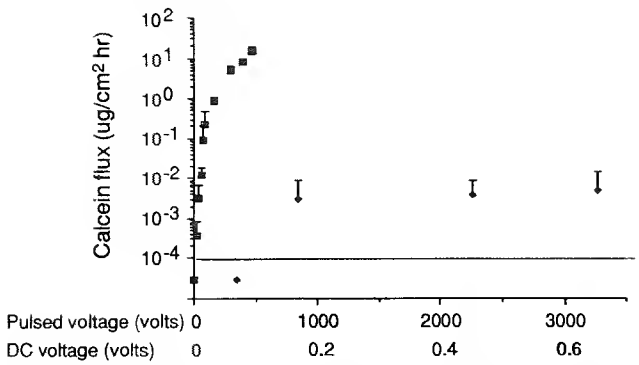

FIG. 3. Transdermal fluxes of calcein during pulsing (■) and during application of dc iontophoresis (♦). Upper axis indicates pulsing voltages electrically "equivalent" to continuous dc voltages on lower axis (see text), suggesting that skin structural changes may be needed to explain the high fluxes caused by electroporation. Each point represents the average of three to seven skin samples, from two to four different subjects. Standard deviation bars are shown. Fluxes below the calcein flux detection limit are indicated below the dashed line.

electroporation literature (7, 8). Upon initial consideration, electron microscopy might also appear to be an appropriate tool for visualizing the pores created by electroporation. However, there currently exist no satisfactory electron micrographs of electropores in any membrane, primarily because electropores are believed to be small (<10 nm), sparse (<0.1% of surface area), and generally short-lived (microseconds to seconds) (7, 8). Thus, it is extremely difficult to visualize electropores by electron microscopy. Moreover, although the name electroporation suggests the creation of physical pores, all that has been concretely established is that a transient high-permeability state is created, characterized by greatly increased permeability and electrical conductivity (7, 8). We therefore did not employ electron microscopy to look for pores in the complex multilaminate structures of the skin, since their existence had not been established in simpler systems.

Enhanced transport of two other polar molecules across the skin was achieved by electroporation: Lucifer yellow (457 Da, −2 charge) and an erythrosin derivative (1025 Da, −1 charge), a small macromolecule, neither of which normally crosses skin at detectable levels. These molecules were selected because they are fluorescent and have different physical properties than calcein. As seen in Fig. 4*A*, pulsing can cause fluxes of both molecules similar to those caused for calcein under the same conditions. This suggests that electroporation-enhanced transport may be broadly applicable to many molecules, possibly including those of higher molecular weights.

We have also observed flux increases due to pulsing of full-thickness human skin, suggesting that artifacts due to epidermis preparation are not significant. However, full-thickness fluxes were delayed (about 1 hr) and were about an order of magnitude lower, probably due to binding or diffusional limitations in the dermis (2–3 mm thick). Moreover, we have observed up to 1000-fold flux increases due to pulsing in frog and hairless rat skin *in vitro* (data not shown).

Finally, electroporation *in vivo* was performed on hairless rats, assessed by measuring serum concentrations of calcein delivered transdermally (Fig. 4*B*). Fluxes in excess of 10 $\mu g/(cm^2 \cdot hr)$ were observed at voltages as low as 30 V; these fluxes are at least 2 orders of magnitude greater than controls (Fig. 4*B*). That the *in vivo* fluxes do not increase with voltage suggests that a rate-limiting step other than transport across the stratum corneum exists, perhaps uptake of calcein from a skin depot into the bloodstream. No visible skin damage

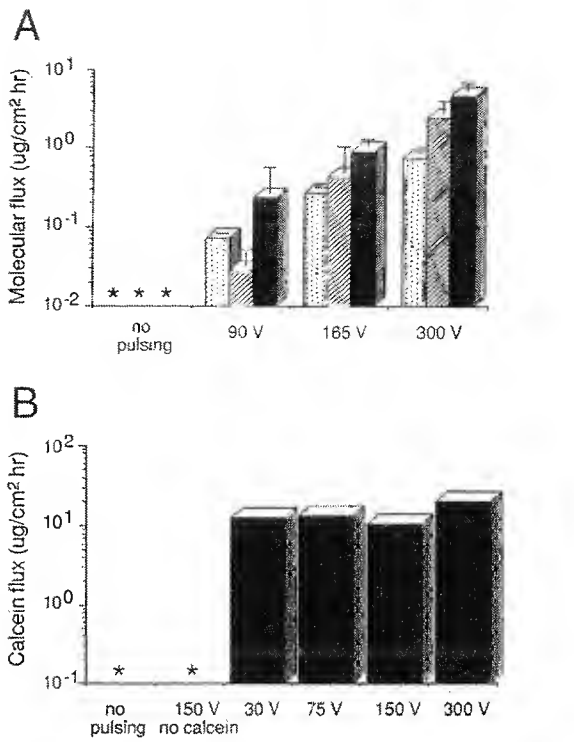

FIG. 4. Transdermal fluxes *in vitro* and *in vivo*. (*A*) Transdermal fluxes of an erythrosin derivative (1025 Da, −1 charge) (stippled bars), Lucifer yellow (457 Da, −2 charge) (hatched bars), and calcein (solid bars) across human skin *in vitro*. This figure demonstrates that electroporation increases the flux of a number of polar molecules having different molecular characteristics. Each point represents the average of three to seven skin samples, from two to four different subjects. Standard deviation bars are shown. Asterisk indicates a flux below the detection limit, of order 10^{-2} $\mu g/(cm^2 \cdot hr)$ for the erythrosin derivative and 10^{-3} $\mu g/(cm^2 \cdot hr)$ for Lucifer yellow. (*B*) Flux of calcein across hairless rat skin *in vivo*, which suggests that electroporation can increase transdermal flux in a living animal. Each point represents the average result from one or two rats. Asterisk indicates a flux below the detection limit, of order 10^{-1} $\mu g/(cm^2 \cdot hr)$.

was observed after pulsing at voltages below 150 V; erythema and edema were evident at higher voltages. Long-term biochemical and pathological studies are needed.

It is well established that the stratum corneum is the primary barrier to transdermal transport (1–4); thus, changes in the stratum corneum probably account for the observed increases in flux due to electroporation. Although it has been applied primarily to living cells, electroporation has also been widely studied in artificial planar bilayer membranes and liposomes (7, 8). Electroporation is a physical process based on electrostatic interactions and thermal fluctuations within fluid membranes; no active transport processes are involved (7, 8). Thus, electroporation could occur in the stratum corneum even though it does not contain living cells.

The stratum corneum has a much higher electrical resistance than other parts of the skin. As a result, an electric field applied to the skin will concentrate in the stratum corneum, resulting in other, viable tissues being exposed to much lower fields. Therefore, under appropriate conditions, an electric field sufficient to cause electroporation could exist in the stratum corneum, while a significantly lower field existed in viable tissues, insufficient to cause electroporation. An implicit targeting mechanism results, where the greatest electric fields are generated where the largest resistivities exist, thereby protecting the already permeable viable parts of the skin and deeper tissues.

It is difficult to state with certainty which electrical conditions will be acceptable for clinical use. Many features,

including pulse voltage/current/energy, pulse length, pulse frequency, duration of total exposure, and electrode size, site, and design, will be important (25). A complete histological examination of the safety of electroporation of skin is beyond the scope of this study. However, that the electrical exposures used were fully reversible over a range of voltages is a strong indication that the procedure is not damaging and may prove to be safe under appropriate conditions. Moreover, there exists a clinical precedent for safely applying electric pulses to skin with voltages up to hundreds of volts and durations up to milliseconds. Such diagnostic and therapeutic applications, which involve stimulation of nerves and may inadvertently cause electroporation of skin, include transcutaneous electrical nerve stimulation, functional electrical stimulation, electromyography, and somatosensory-evoked-potential testing (25, 26).

Because of the stratum corneum's overall hydrophobic character and net negative charge, transdermal transport of negatively charged hydrophilic molecules is especially challenging (2, 3). Calcein, with eight charge sites and a net charge of −4 (19), is therefore considerably more difficult to transport across the skin than many other molecules. Approaches to transdermal flux enhancement involving chemical enhancers have been successful with some lipophilic and moderately polar molecules but are limited in applicability to highly polar and charged molecules (2–4). Iontophoresis has been successfully employed with some polar and charged molecules (2–4). For many drugs, delivery rates in the range of micrograms per square centimeter per hour could be therapeutic, whereas significantly higher rates of delivery may be required for other drugs (2, 3). In general, a 10-fold increase in flux caused by an enhancement method is impressive, and a 100-fold increase is of great interest. Thousandfold increases are rarely found (2, 3). The increases of up to 10,000-fold in flux that are caused by electroporation are therefore potentially very significant and could make possible transdermal delivery of many drugs at therapeutic levels.

Finally, transdermal flux enhancement has been demonstrated with other methods, including chemical, iontophoretic, and ultrasonic (2–4). Because electroporation is mechanistically different, involving temporary alterations of skin structure, it could be used in combination with these or other enhancers. Electroporation may also be useful in other applications involving transport across skin, such as noninvasive sensing for biochemical measurement, gene therapy, and cancer chemotherapy. Together, these results suggest that electroporation of mammalian skin occurs and may be useful as a mechanism to enhance transdermal drug delivery.

We thank C. S. Lee, J. C. Pang, K. Markle, A. A. Kon, D. S. Seddick, R. P. Marini, F. J. Schoen, R. O. Potts, R. H. Guy, and S. K. Burns for assistance and discussions and the Departments of Pathology at Beth Israel, Brigham and Women's, and Massachusetts General Hospitals and the National Disease Research Interchange for tissue acquisition. This research was supported in part by Cygnus Therapeutic Systems (M.R.P., V.G.B., and J.C.W.), Army Research Office Grant DAAL03-90-G-0218 (V.G.B. and J.C.W.), and National Institutes of Health Grants GM34077 (J.C.W.) and GM44884 (R.L.).

1. Champion, R. H., Burton, J. L. & Ebling, F. J. G., eds. (1992) *Textbook of Dermatology* (Blackwell, London).
2. Bronaugh, R. L. & Maibach, H. I., eds. (1989) *Percutaneous Absorption, Mechanisms—Methodology—Drug Delivery* (Dekker, New York).
3. Hadgraft, J. & Guy, R. H., eds. (1989) *Transdermal Drug Delivery: Developmental Issues and Research Initiatives* (Dekker, New York).
4. Cullander, C. & Guy, R. H. (1992) *Adv. Drug Delivery Rev.* 8, 291–329.
5. Bouwstra, J. A., de Vries, M. A., Gooris, G. S., Bras, W., Brussee, J. & Ponec, M. (1991) *J. Controlled Release* **15**, 209–220.
6. Elias, P. M. (1991) *J. Controlled Release* **15**, 199–208.
7. Neumann, E., Sowers, A. E. & Jordan, C. A., eds. (1989) *Electroporation and Electrofusion in Cell Biology* (Plenum, New York).
8. Chang, D. C., Chassy, B. M., Saunders, J. A. & Sowers, A. E., eds. (1992) *Guide to Electroporation and Electrofusion* (Academic, New York).
9. Okino, M. & Mohri, H. (1987) *Jpn. J. Cancer Res.* **78**, 1319–1321.
10. Powell, K. T., Morgenthaler, A. W. & Weaver, J. C. (1989) *Biophys. J.* **56**, 1163–1171.
11. Mir, L. M., Orlowski, S., Belehradek, J. & Paoletti, C. (1991) *Eur. J. Cancer* **27**, 68–72.
12. Titomirov, A. V., Sukharev, S. & Kistanova, E. (1991) *Biochim. Biophys. Acta* **1088**, 131–134.
13. Gummer, C. L. (1989) in *Transdermal Drug Delivery: Developmental Issues and Research Initiatives*, eds. Hadgraft, J. & Guy, R. H. (Dekker, New York), pp. 177–186.
14. Friend, D. R. (1992) *J. Controlled Release* 18, 235–248.
15. Suzuki, H. K. & Mathews, A. (1966) *Stain Technol.* **41**, 57–60.
16. Sontag, W. (1980) *Calcif. Tissue Int.* **32**, 63–68.
17. Wagner, J. G. (1975) *Fundamentals of Clinical Pharmacokinetics* (Drug Intelligence Publ., Hamilton, IL).
18. Goldstein, L., ed. (1977) *Introduction to Comparative Physiology* (Holt, Rinehart and Winston, New York).
19. Furry, J. W. (1985) *Preparation, Properties and Applications of Calcein in a Highly Pure Form* (Iowa State Univ. Press, Ames, IA).
20. Benz, R. & Zimmermann, U. (1980) *Bioelectrochem. Bioenerg.* **7**, 723–739.
21. Hibino, M., Shigemori, M., Itoh, H., Nagayama, K. & Kinosita, K. (1991) *Biophys. J.* **59**, 209–220.
22. Weaver, J. C. & Barnett, A. (1992) in *Guide to Electroporation and Electrofusion*, eds. Chang, D. C., Chassy, B. M., Saunders, J. A. & Sowers, A. E. (Academic, New York), pp. 91–118.
23. Wearley, L., Liu, J. C. & Chien, Y. W. (1989) *J. Controlled Release* **9**, 231–242.
24. Green, P., Shroot, B., Bernerd, F., Pilgrim, W. R. & Guy, R. H. (1992) *J. Controlled Release* **20**, 209–218.
25. Reilly, J. P. (1992) *Electrical Stimulation and Electropathology* (Cambridge Univ. Press, New York).
26. Webster, J. G., ed. (1988) *Encyclopedia of Medical Devices* (Wiley, New York).

Biophysical Journal Volume 67 July 1994 42–56

Theory of Electroporation of Planar Bilayer Membranes: Predictions of the Aqueous Area, Change in Capacitance, and Pore-Pore Separation

Scott A. Freeman,* Michele A. Wang,* and James C. Weaver‡

*Department of Physics and ‡Harvard-M.I.T. Division of Health Sciences and Technology, Massachusetts Institute of Technology, Cambridge, Massachussetts 02139 USA

ABSTRACT A large increase in the transmembrane voltage, $U(t)$, of a fluid bilayer membrane is believed to result in the occurrence of temporary aqueous pathways ("pores") across the membrane. The number, size, and evolution dynamics of these pores are expected to be crucial to the transport of water-soluble species ranging from small ions to macromolecules such as proteins and nucleic acids. In this paper we use a transient aqueous pore theory to estimate the fraction of the membrane area, $F_w(t)$, which is temporarily occupied by water-filled pores for short square, exponential, and bipolar square pulses. For short pulses, "reversible electrical breakdown" occurs when the transmembrane voltage reaches about 1 V, and $F_w(t)$ is predicted to rise rapidly, but always to be less than 10^{-3}. The conductance of a large number of pores causes reversible electrical breakdown and prevents a significantly larger U from being reached. Despite the large dielectric constant of water, for reversible electroporation the associated change in membrane capacitance, ΔC, due to the pores is predicted to be small. Moreover, for a flat membrane the minimum value of the mean pore-pore separation is large, about 60 times the minimum pore radius. In flat membranes, pores are predicted to repel, but the opposite is expected for curved cell membranes, allowing the possibility of coalescence in cell membranes. For some moderate values of U, rupture (irreversible electrical breakdown) occurs, as one or more supracritical pores expand to the membrane boundary and the entire membrane area becomes aqueous. In all cases it is found that a quantitative description of electroporation requires that a pore size distribution, rather than a single size pore.

INTRODUCTION

Electroporation is increasingly used for the introduction of water-soluble molecules into cells and has many potential applications in biology and medicine (Neumann et al., 1989; Tsong, 1991; Chang et. al., 1992; Blank, 1993; Weaver, 1993a, b; Orlowski and Mir, 1993). Although the mechanism by which this occurs is incompletely understood, it is generally believed that a rapid structural rearrangement of the membrane occurs, whereby many aqueous pathways ("pores") perforate the membrane. One class of electroporation theories is based on transient aqueous pores that are explicitly assumed to be created by the combined effects of thermal fluctuations and the local electric field across the membrane. The first version of transient aqueous pore theories was presented by Chizmadzhev and co-workers in a series of seven back-to-back papers, of which only the first is cited here (Abidor et al., 1979). In the present paper we estimate the extent of membrane poration by using a recent version of a transient aqueous pore theory (Barnett and Weaver, 1991). This allows estimation of the total aqueous area (expressed here as a fraction, F_w), the change in membrane capacitance due to the pores, and the mean separation between the pores. The latter is relevant to the possibility that pores coalesce to form "cracks" or other larger openings in the membrane (Sugar et al., 1987).

Planar bilayer membranes have often been used to investigate basic aspects of the lipid bilayer component of cell membranes. In the case of cell membrane electroporation, it is likely that most of the poration is localized to the relatively small region for which the transmembrane voltage, $U(t)$, is largest. For example, in the case of an isolated spherical cell, electroporation is believed to occur mainly at the "polar caps" of the cell. Indeed, there is experimental support for this, based on fluorescence measurements that respond to the local transmembrane voltage (Hibino et al., 1991). It is plausible, therefore, that such local regions can be reasonably approximated by sections of planar membrane that experience the same $U(t)$, and this further motivates the present study.

MATERIALS AND METHODS

We have slightly modified a previous theoretical model (Barnett and Weaver, 1991; Weaver and Barnett, 1992) by rewriting the computer code to provide greater flexibility in what can be computed. As a consequence, simulation of electroporation due to an exponential pulse or bipolar square pulse in addition to a square pulse was made possible. We then carried out several calculations of electrical behavior, the dynamic, heterogeneous pore population, and quantities dependent on the pore population. A detailed

Received for publication 13 July 1992 and in final form 23 February 1994.

Address reprint requests to James C. Weaver, Division of Health Sciences & Technology, Biomedical Engineering Center, Room 20A-128, Massachussetts Institute of Technology, Cambridge, MA 02139. Tel.: 617-253-4194; Fax: 617-253-2514.

S. Freeman's present address: Department of Physics, University of Michigan.

M. Wang's present address: Department of Architecture, University of Washington.

0006-3495/94/07/42/15 $2.00

presentation of the basic model (Barnett and Weaver, 1991; Weaver and Barnett, 1992) is too lengthy to include here. Key features are briefly described, the Appendix provides a discussion of the origin of some of the parameters, and a complete listing of the notation and the values of fixed parameters is given in Table 1.

We begin with the estimate of the free energy change, ΔE, associated with forming a pore of radius r if the spatially averaged transmembrane voltage is $U(t)$:

$$\Delta E(r, U) = 2\pi\gamma r - \pi\Gamma r^2 - \frac{\pi(K_w - K_l)U^2}{h}\int_{r_{min}}^{r} \alpha^2 r\, dr, \qquad (1)$$

where the effects of inhomogeneous electric fields near the pore entrances, Born energy repulsion of ions, and hindered drift motion within the pore are subsumed into the function $\alpha(r)$

$$\alpha(r) = \left[1 + \frac{\pi r\sigma_p(r)}{2h\sigma_e}\right]^{-1}. \qquad (2)$$

Here σ_p is the reduced conductivity within a pore, and σ_e is the bulk solution conductivity. The appearance of a heterogeneous pore population in response to the occurrence of elevated U is governed by a phenomenological estimate of the pore creation rate

$$(\dot{N})_c = \nu_0 V_m \exp\left(-\frac{\delta_c - aU^2}{kT}\right). \qquad (3)$$

Here $\nu = \nu_0$, V_m is the attempt rate, ν_0 is an attempt rate density, and $V_m = hA_m$ is the membrane volume (Weaver and Mintzer, 1981). Although not understood in detail, it is assumed that an energy barrier, $\Lambda = \delta_c - aU^2$, must be overcome to form a pore. Other estimates of the barrier (Glaser et al., 1988) could be incorporated in future versions, but to maintain consistency with our previous work (Barnett and Weaver, 1991), the previously employed barrier is again used here. Pores are also assumed to disappear, but are destroyed only when they shrink to their minimum allowed radius, r_{min}. The destruction process is assumed to be independent of U. Specifically, the total rate of pore destruction is

$$(\dot{N})_d = \chi n(r_{min})\exp\left(-\frac{\delta_d}{kT}\right), \qquad (4)$$

where δ_d is a fixed barrier, and χ (Table 1) is a constant with dimensions of velocity. Once pores have formed their expansion and contraction is governed by Smoluchowski's equation

$$\frac{\partial n}{\partial t} = D_p\left(\frac{\partial^2 n}{\partial r^2} + \frac{\partial}{\partial r}\left(\frac{n}{kT}\frac{\partial \Delta E}{\partial r}\right)\right) \qquad (5)$$

The function $n(r, t)$ is a pore probability density function, such that the instantaneous number of pores with radii between r and $r + \Delta r$ is $n(r, t)\Delta r$. This governs the evolution of $n(r, t)$, the pore probability density function, in response to changes in ΔE caused by a changing transmembrane voltage, $U(t)$, through Eq. 1 (Figs. 3, 7, and 11).

This differential equation is implicitly coupled to a first order differential equation that describes the interaction of the membrane with its environment, i.e., the charging of the membrane through the bathing electrolyte from the pulse generator (Fig. 1). After the pulse ends, the generator is disconnected from the system so that the membrane can then discharge only by moving ions across the membrane through pores (Figs. 2, 6, and 10).

$$C\frac{dU}{dt} = \begin{cases} \dfrac{IR_N}{R_E + R_N} - U\left(G(t) + \dfrac{1}{R_E + R_N}\right) & \text{if } t < t_{pulse} \\ -UG(t) & \text{if } t > t_{pulse} \end{cases} \qquad (6)$$

Here I is the instantaneous current flowing through the membrane, which depends on the pore sizes, the local, decreased transmembrane voltages (because of the spreading resistance), and the reduced conductivity within the pores. Equations 3–6 together determine the evolution of the pore population and its electrical interaction with the membrane's environment. Other ingredients and inputs such as the physical models for pore conduction, the rates of pore creation and of pore destruction (at r_{min}), and the pulse magnitude and shape then can be varied.

Both mechanical and electrical behavior are relevant. A planar membrane can rupture (mechanical destruction) by acquiring one or more supracritical pores (Abidor et al., 1979; Weaver and Mintzer, 1981; Sugar, 1981; Toner and Cravalho, 1990). Alternatively, a planar membrane can protect itself against rupture by rapidly acquiring so many small pores that a very large membrane conductance is achieved, which quickly discharges the membrane before any supracritical pores can evolve (Powell et al., 1986; Barnett and Weaver, 1991; Weaver and Barnett, 1992). The appearance of a heterogeneous pore population is fundamental to the transient aqueous pore model and is described by a pore probability density function, $n(r, t)$, which is obtained as a solution of Eq. 5 (Figs. 3, 7, and 11).

Partial insight into the pore population can be gained by considering the average pore radius, $\bar{r}(t)$, which is straightforwardly computed as

$$\bar{r}(t) = \frac{1}{N_p(t)}\int_{r_{min}}^{\infty} rn(r, t)\, dr, \qquad (7)$$

where the instantaneous total number of pores in the membrane is

$$N_p(t) = \int_{r_{min}}^{\infty} n(r, t)\, dr. \qquad (8)$$

Typical predicted behavior for short square, exponential, and bipolar square pulses is shown in Figs. 4, 8, and 12.

The total pore area at the midplane of the membrane is similarly estimated. In the transient aqueous pore theories to date, including the present version, a very simple, circular cylinder geometry has been used to represent

TABLE 1 Notation and values of parameters

Parameter		Value
a	coefficient of U^2 in A	1.9×10^{-20} F
A_m	Membrane area ($\pi R^2_{sperture}$)*	1.45×10^{-6} m^2
C_0	C, the capacitance of membrane at $U = 0$	9.61×10^{-9} F
D_p	Diffusion constant in pore radius space*	5×10^{-14} m^2 s^{-1}
$G(t)$	Membrane conductance	Initially almost zero
h	Membrane thickness*	2.8 nm
kT	Boltzmann's constant times temperature	4×10^{-21} J
K_l	Dielectric constant of lipid*	2.1
K_w	Dielectric constant of water	80
R_E	Series resistance of electrolyte, electrodes, and wires	30 Ω
R_N	Internal resistance of current source (pulse generator)	50 Ω
$R(t)$	Membrane resistance ($1/G(t)$)	Initially almost infinite
r_{max}	Large pore initial size	40 nm
r_{min}	Minimum pore radius*	1 nm
γ	Pore edge energy density*	2×10^{-11} J m^{-1}
Γ	Membrane surface energy*	1×10^{-3} J m^{-2}
δ_c	Voltage-independent barrier to pore formation*	2×10^{-19} J
δ_d	Pore destruction energy barrier*	2×10^{-19} J
ϵ_0	Permittivity of free space	8.85×10^{-12} F m
Δr	Numerical grid spacing of simulation	0.026 nm
χ	Pore destruction rate prefactor*	5×10^{16} m s^{-1}
ν	Pore creation rate prefactor*	10^{28} s^{-1}
σ_e	Conductivity of bulk solution	9.8 S m^{-1}

* Parameters characterizing the membrane. Many features of the basic model and its parameters have been published previously (Barnett and Weaver, 1991).

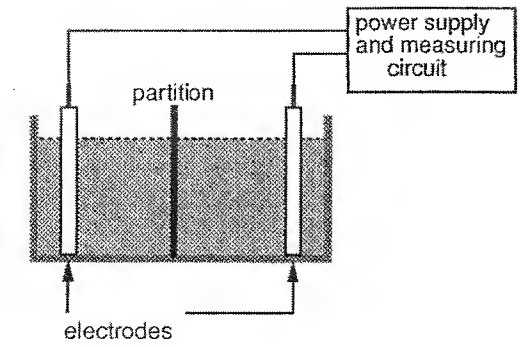

(a)

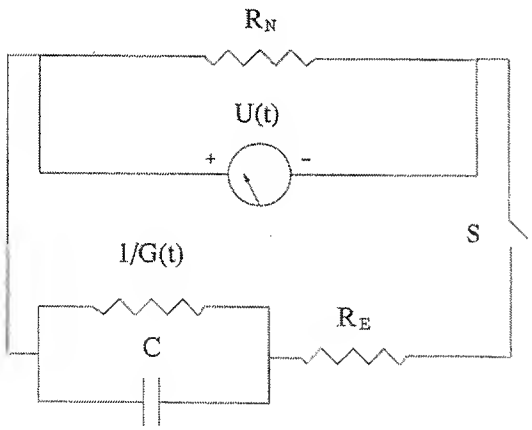

(b)

FIGURE 1 Equivalent circuit that represents the planar membrane and the external environment (experimental apparatus). The resistor, R_E, represents the combined resistance of (1) the bulk electrolyte separating the membrane from the electrodes, (2) any constant electrolyte/electrode interfacial resistance, and (3) the pulse generator output resistance. Conceptually, the generator develops a voltage, $V(t)$, which is applied to the membrane system by closing the switch, S. At the end of the pulse, the switch is instantaneously opened, so that the membrane can only discharge through the membrane. The membrane is represented by an essentially constant capacitance, C, and time-dependent resistance, $R(t)$. The membrane conductance, $G(t) = 1/R$, is attributed to the instantaneous sum of the conductances of all the individual transient pores. Consistent with this approach, the transient pore population is described by a probability density function, $n(r,t)$, which appears in Eq. 5, such that $n(r, t)\Delta r$ is the average number of pores with radii between r and $r + dr$ at time t. The instantaneous transmembrane voltage, $U(t)$, is described by Eq. 6. These general features are unchanged from the previous version of the theoretical model (Barnett and Weaver, 1991). The approximation that C is constant is here found to be consistent with the behavior of the present model, as was estimated in a much earlier model that treated the worst case of a membrane saturated with pores (Weaver et al., 1984).

a pore. Here the aqueous area, $A_w(t)$, of the membrane was estimated by computing the total cross sectional areas of the pores.

$$A_w(t) = \int_{r_{min}}^{\infty} \pi r^2 n(r, t)\, dr \tag{9}$$

The total membrane area, $A_m = \pi R^2_{aperture}$, is considered to be the sum of lipid area and aqueous area. As pores form in a planar membrane that exists across a macroscopic aperture, the excess membrane material is believed eventually to be transferred to the edge of the aperture. This interpretation is central to the idea that rupture occurs by expansion of one or more supracritical pores so that all of the membrane material reaches the aperture. When this occurs, the "membrane" is entirely aqueous, and is therefore regarded as destroyed. However, for short times transfer of membrane material over the distance $\approx R_{aperture}$ cannot be valid. Instead, local accumulation of material and local thickening of the membrane is a more likely immediate outcome of pore formation. In the spirit of an order of magnitude estimate, excess membrane material near a pore can be expected to remain localized for times less than $t_{local} \approx R_{aperture}/v_{sound}$. Here $v_{sound} \approx 1.5 \times 10^3$ m s^{-1} is estimated by using the speed of sound in water and in oil. For the membrane used here ($R_{aperture} \approx 7 \times 10^{-4}$ m), this gives $t_{local} \approx 5 \times 10^{-7}$ s, which is on the same time scale as REB. Thus, for times shorter than t_{local}, excess membrane material probably accumulates locally, resulting in locally thicker regions of the membrane. However, local thickening of portions of the lipid area of the membrane does not affect the aqueous area of the membrane due to pores. When expressed as an aqueous fractional area, $F_w(t)$, this is

$$F_w(t) = \frac{A_w(t)}{A_m} \tag{10}$$

The transient aqueous pore theories to date have assumed that the membrane capacitance, C, is constant (Fig. 1). One experimental observation of electroporation supports this (Chernomordik et al., 1982). Here this assumption is tested by estimating the change in C that is due to the appearance of the aqueous pores, i.e., by regarding each pore as a microscopic capacitor in which the relevant dielectric constant is that of bulk water ($K_w = 80$). This estimate neglects the contribution of bound water at the interior surfaces of pores (Weaver et al., 1984). Bound water has a smaller dielectric constant (e.g., $K_{bw} \approx 6$–10), so that the present estimate of ΔC should be conservative, i.e., an overestimate of the pores' contribution to C. Neglect of the previously mentioned local thickening of the membrane will also contribute to an overestimate of ΔC, because these thicker regions will cause a reduction in capacitance. However, because the dielectric constant of lipid is $K_l \approx 2$ and that of the aqueous pore is $K_2 \approx 80$, the contribution of the pores to ΔC will be far larger than that by local thickened regions. For this reason, the contribution of the thicker lipid regions can be neglected. In this approximation, the total membrane capacitance is the sum of its lipid contribution at fixed thickness, C_l, and of the water-filled pores, C_w.

$$C(t) \approx C_l + C_w = \frac{K_l \epsilon_0 (A_m - A_w(t))}{h} + \frac{K_w \epsilon_0 A_w(t)}{h}; \quad A_m \approx \text{constant} \tag{11}$$

If significant electroporation occurs, the contribution to ΔC may be due mainly to pores. This is in contrast to the situation at small transmembrane voltages where only a few pores are created, and where electrostriction (electrically caused decrease in h) appears to be the dominant mechanism. The fractional change associated with the appearance of pores is

$$\frac{\Delta C(t)}{C} \approx \left(\frac{K_w}{K_l} - 1\right)\frac{A_w(t)}{A_m} \approx [39]F_w(t) \tag{12}$$

Thus, the time dependence of $C(t)$ due to pores is the same as $F_w(t)$. For this reason, only F_w is presented in Figs. 5, 9, and 13. Multiplication of the maximum value of $F_w(t)$ found there by $K_w/K_l - 1 = 39$ shows that the maximum fractional change in capacitance for reversible electroporation at large transmembrane voltages is less then 2%. We emphasize that these estimates of the pore contribution are overestimates, because the contribution of localized membrane thickening and bound water within pores are both neglected.

The average spacing between pore centers, $\bar{S}_{pp}$, was estimated by assuming that pore formation occurs randomly with respect to position in the membrane. The area density of pores within the membrane is $\delta_p(t) = N_p(t)/A_m$. We used a polar coordinate system that was fixed at the center of a first pore. The probability of a second pore being located within the

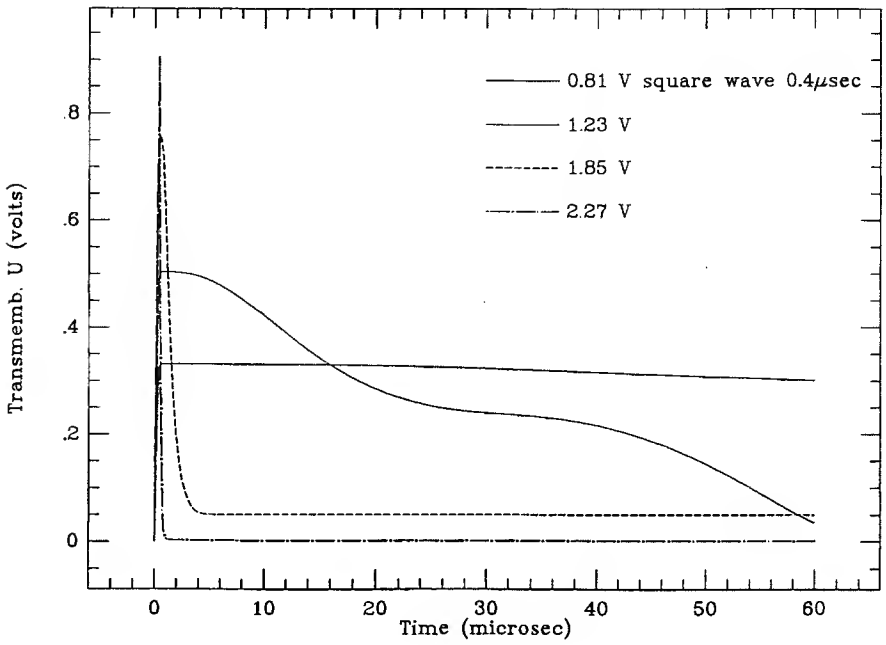

FIGURE 2 Predicted square pulse behavior of the transmembrane voltage, $U(t)$, due to a single 0.4-μs pulse of the indicated amplitudes. As found previously, four distinguishable outcomes are possible: (1) simple charging of the membrane capacitance (smallest pulse; here 0.81 V), (2) rupture of the membrane (larger pulse; here 1.23 V), (3) incomplete reversible electrical breakdown (still larger pulse; here 1.85 V), (4) reversible electrical breakdown (REB) (largest pulse; here 2.27 V). The electrical behavior predicted by a recent transient aqueous pore model (Barnett and Weaver, 1991) agrees reasonably, but not exactly, with experimental observations of these outcomes (Benz et al., 1979).

annulus between s and $s + ds$ from the center of the first pore is

$$P_{1\text{ in annulus}}(s)ds = 2\pi\delta_p(t)sds \tag{13}$$

where it was assumed that ds is sufficiently small that the probability of finding the center of a second pore in an annulus of thickness ds is much less than unity. This is appropriate because pores are rare events within the membrane. The probability P_1 was multiplied by the probability of finding zero pores in a disk of radius s centered at the first pore. According to Poisson statistics (appropriate for rare events) this second probability is

$$P_{0\text{ in disk}}(s) = P(n, \bar{n}(s)) = \frac{\bar{n}(s)^n e^{-\bar{n}(s)}}{n!} \tag{14}$$

where $\bar{n}(s)$ is the the mean number of pores in a disk of radius s, i.e., $\bar{n}(s) = \delta_p\pi s^2$. The probability of the second pore being located between s and $s + ds$ from the origin, therefore, is given by

$$P(s)ds = P_{0\text{ in disk}}(s)P_{1\text{ in annulus}}(s)ds = \frac{(\delta_p\pi s^2)^0 e^{-\pi s^2\delta_p}}{0!} 2\pi\delta_p sds \tag{15a}$$

$$= 2\pi\delta_p se^{-\delta_p\pi s^2}ds. \tag{15b}$$

To find the mean separation between pore centers, we then computed

$$\bar{S}_{pp}(t) = \int_0^\infty sP(s)\,ds = 2\pi\delta_p(t)\int_0^\infty s^2 e^{-\pi\delta_p(t)s^2}\,ds = \frac{1}{2}\left[\frac{1}{\delta_p}(t)\right]^{1/2}. \tag{16}$$

The largest number of pores, and the smallest pore separation, occurs for pulses that cause REB. In a typical REB simulation, it is predicted that approximately 10^8 pores occur in the membrane of area $A_m = 1.45 \times 10^{-6}$ m^2, which gives $\delta_p = 1.45 \times 10^{14}$ pores m^{-2}, and a mean pore spacing of 60 nm. As shown in the figures, during reversible electroporation caused by a short pulse most of the pores are small. Thus, the mean pore spacing is much larger than the diameter of a typical pore. However, during rupture many fewer pores appear, and the behavior is dominated by one or a small number of expanding supracritical pores.

DISCUSSION

Creation of aqueous pathways ("pores") is central to the concept of electroporation. Such pores are hypothesized to allow small ions to cross the membrane so that the electrical conduction of the membrane, $G(t)$, can change by orders of magnitude. Although the structure of transient aqueous pores has been suggested in drawings, their actual structure remains unknown. Because of the transient nature of the pores, and the basis of contrast and spatial resolution in known types of microscopy, such pores are not likely to be directly visualized (Weaver, 1993b). Instead, their structure must be inferred. Here we have shown that use of a transient aqueous pore theory that (1) is constructed from continuum physical representations, and (2) is consistent with known electrical behavior of artificial planar bilayer membranes, leads to the view that only a small fraction of the membrane is occupied by pores. This, in turn, places a bound the magnitude of ΔC, and on the minimum value of $\bar{S}_{pp}$. Similarly, the average spacing of pores was estimated and found to be large, even during reversible electrical breakdown when the largest number of pores are present. Specific predictions of the model are discussed below.

Transmembrane voltage behavior

The model makes specific predictions of $U(t)$, and these have been previously presented (Barnett and Weaver, 1991). The electrical behavior due to a short (0.4 μs) square pulse was the subject of an early experimental study using a planar oxidized cholesterol membrane (Benz et al., 1979). As discussed previously, the transient aqueous pore theory predictions are in reasonable agreement with most features of these measurements. Similar planar membrane experiments using exponential and bipolar square pulses apparently have not yet been carried out. Exponential pulses are widely used with cell experiments, but

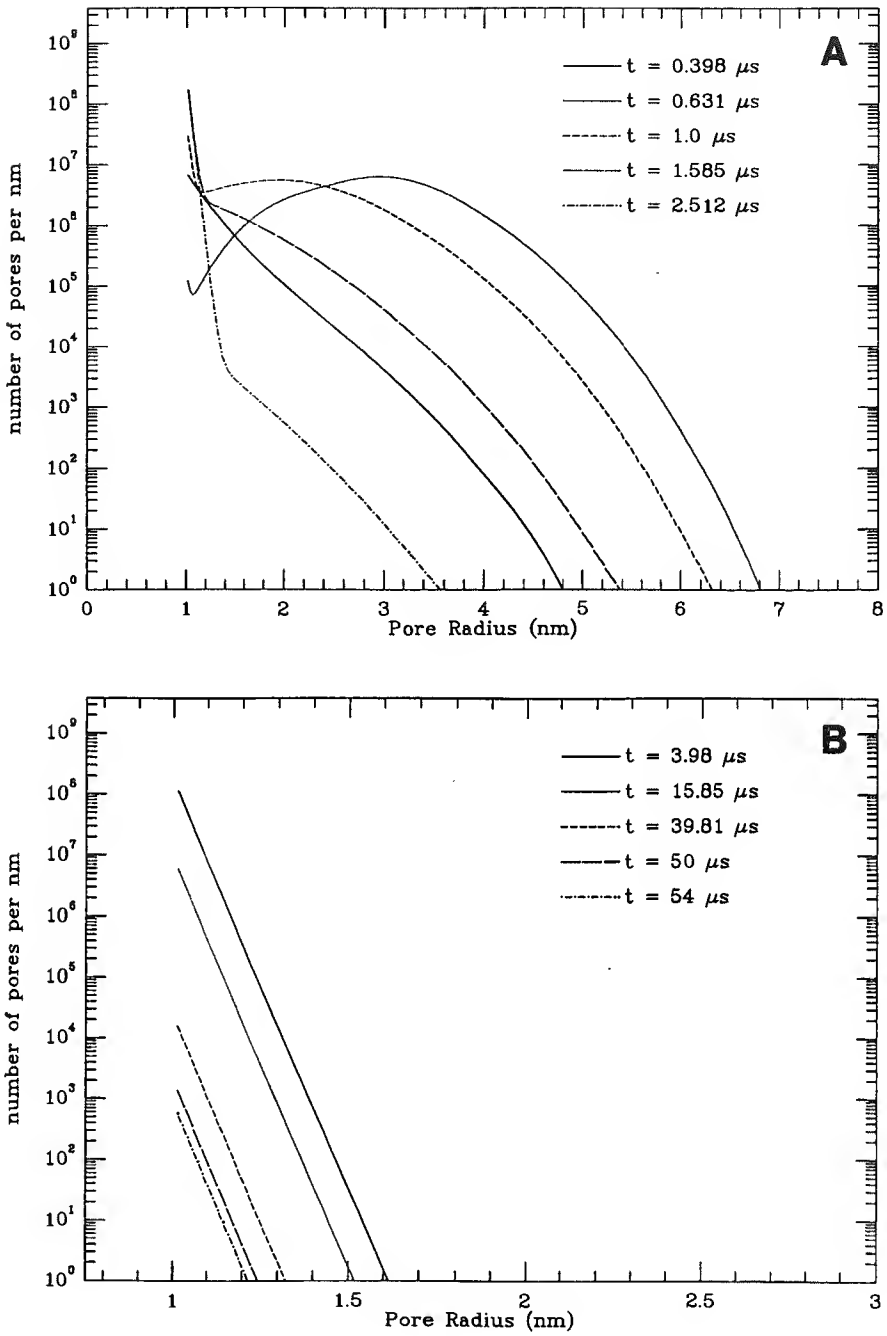

FIGURE 3 Pore population evolution with time for a typical case involving REB (here the 2.27 V square pulse of Fig. 2). The population is described by a probability density function, $n(r, t)$, such that the number of pores with radii between r and $r + dr$ is $n(r, t)dr$. For the graphs shown here, a finite "bin width" of $\Delta r = 0.026$ nm was used instead of dr. Each of the curves is labeled with the time after the start of the pulse. At $t = 0$ very few (about 6) pores are present. As the pore population evolves because of a pulse, new pores are created at the minimum pore radius, $r_{min} = 1.0$ nm, and tend to expand because of the reduced pore formation energy at larger U. As inspection shows, for the larger pulses very large numbers of pores are predicted to rapidly appear, with some reaching large (e.g., 4 nm) sizes. Although the rapidly changing pore population distribution cannot be directly observed, it underlies the electrical behavior of Fig. 2. (*A*) $n(r, t)$ plots for $t = 0.398$ to 2.512 μs. Note that the plot "peaks" after the 0.4-μs pulse ends. (*B*) For $t = 3.98$–54 μs.

usually their time constants are much longer (10^{-4} to 10^{-2} s). Such long pulses have a high probability of rupturing planar membranes and, therefore, are not expected to be particularly worthwhile choices for the planar case. In contrast, vesicles have no meniscus and are not expected to rupture in this way (Sugar and Neumann, 1984), so much longer pulses should be tolerated. The mechanism of cell membrane destruction is less clear. If other cell structures (e.g., cytoskeleton) act to provide boundaries for portions of the membrane, these portions may act like planar membranes and, therefore, be subject to prompt rupture. If not, the cell membrane may behave like a vesicular membrane and not rupture. With this in mind, the planar membrane is relevant to both artificial planar membranes and portions of cell membranes.

Heterogeneous, dynamic pore populations

Although $n(r, t)$ cannot be measured directly, it underlies the functions $U(t)$ and $G(t)$, which can be experimentally determined. Significantly, however, different types of electroporation phenomena appear to be primarily due to different size pores. Specifically, rupture is due to a small number (only one is needed) of large pores, whereas reversible electrical breakdown is due to a large number of small pores. Thepore population may also play a sieving role in molecular

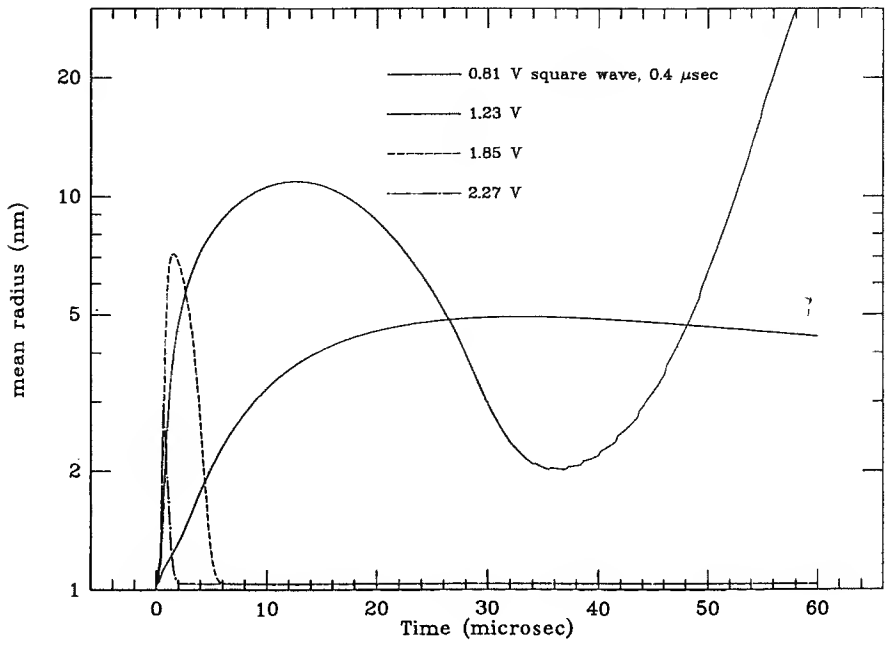

FIGURE 4 Predicted mean pore radius as a function of time, $\bar{r}(t)$, for the four square pulse amplitudes of Fig. 2. The density function appearing in Eq. 5 (Fig. 3) was used to compute the arithmetic average value (Eq. 7). Note that $\bar{r}$ changes markedly with pulse amplitude. For small U, the average values are large, but very few pores are present. For example, rupture involves one or a small number of supracritical pores, which can expand until the membrane boundary is reached. At large U, there are many more pores, but most are small. These contribute to the conductance of small ions across the membrane, and underly the protective process of "reversible electrical breakdown," which is really not breakdown, but instead, the onset of massive ionic conductance that discharges the membrane.

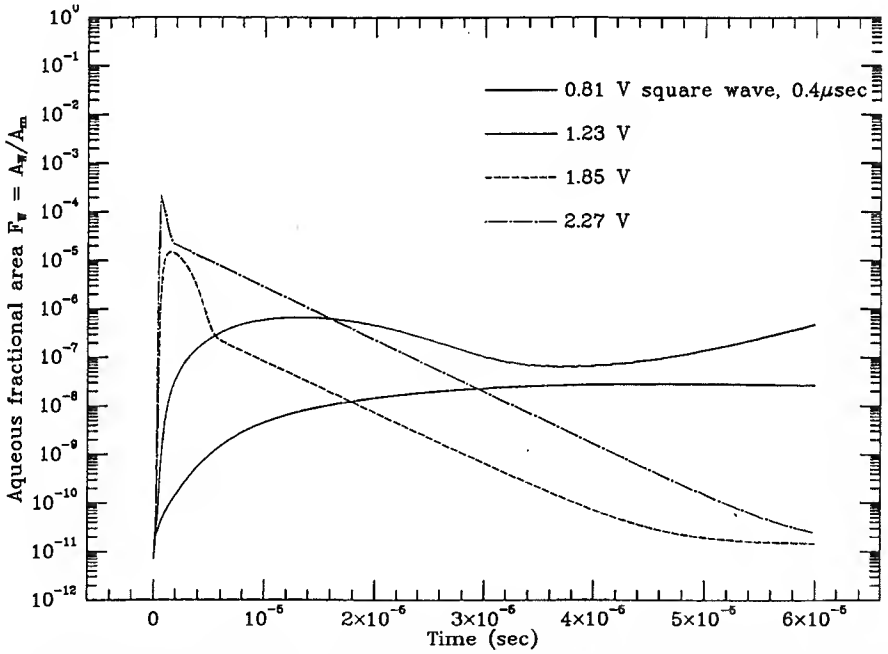

FIGURE 5 Aqueous fractional area of the membrane, $F_W(t) = A_w(t)/A_m$, as a function of time for several different magnitude 0.4 μs square pulses. These plots were obtained by computing the pore population distribution (e.g., Fig. 3), summing the individual pore cross sectional areas, $A_p(r) = \pi r^2$, and dividing by the total membrane area, A_m. A realistic value, $A_m = 1.45 \times 10^{-6}$ m^2, for an artificial planar bilayer membrane was used. Note that the maximum value of F_W is approximately 10^{-3}, i.e., only a small fraction of the membrane is actually occupied pores. Nevertheless, these dominate the transport properties of the membrane, here represented by the massive ionic conductance that is responsible for "reversible electrical breakdown." For pulses that cause REB, the behavior of $F_w(t)$ is nearly the same as $N_p(t)$, the total number of pores (Barnett and Weaver, 1991), because most pores are close to r_{min}. Moreover, the predicted fractional change in membrane capacitance, $\Delta C(t)/C$, exhibits essentially the same behavior as $F_w(t)$, differing only by a proportionality factor (see Eq. 10). As illustrated by the 0.81-V pulse, small pulses cause capacitance changes that are essentially complete within 30 μs.

transport. If so, the presence of progressively fewer pores at larger radii will play an important role in governing how molecular transport decreases as molecular size increases (Weaver and Barnett, 1992). This suggests that theoretical models that involve only a single size pore will be incomplete and, therefore, misleading.

Mean pore radius behavior

Partial characterization of the pore population during electroporation is obtained by considering the average radius, $\bar{r}(t)$. As shown in Figs. 4, 8, and 12, there are significant changes in the behavior of $\bar{r}(t)$ as the pulse amplitude of

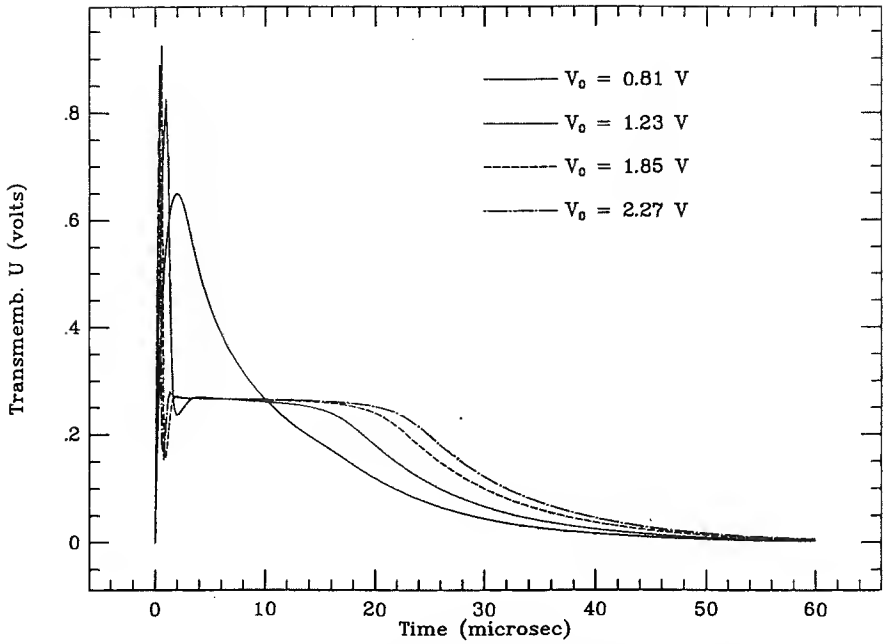

FIGURE 6 Transmembrane voltage, $U(t)$, for four exponential pulses such that $V = V_0 e^{-t/\tau}$ is supplied by the pulse generator (Fig. 1). The same amplitudes, V_0, as for the square pulses of Fig. 2 were used. Again note that the maximum value of U is about 1 V. The time constant, τ = 10 μs, is considerably larger than the width of the square pulse, so that the membrane is exposed to large U for longer times that in Fig. 2. With this in mind, note the behavior of U the three larger pulses: (1) REB occurs within the first μs, resulting in a sudden drop in U, (2) a resumption of membrane charging then occurs (but the membrane now has a much lower resistance), (3) the same temporary plateau is reached by all three pulses for more than 10 μs, and a relaxation of U occurs with similar, but not identical, characteristic times. This is not rupture (see Figs. 4 and 5), but a response of the electroporated membrane to decreasing pulses of the different amplitudes. Note the rapid charging, early occurrence of REB (the large "spikes" to the left), and the approximate plateau beginning at about 2 μs to about 15–24 μs.

the three types of pulses is increased. The evolution of large $\bar{r}(t)$ at moderate U clearly hints at rupture. However, the rapid emergence of small $\bar{r}(t)$ followed by $\bar{r}(t) \rightarrow r_{min}$, in itself, does not adequately describe reversible electrical breakdown. In general, large increases in U caused by short pulses favor more small than large pores. However, all versions of transient aqueous pore theories to date have used a constant edge energy, γ, although it has been recognized that $\gamma = \gamma(r)$, with a strong r dependence expected for small pores (Weaver and Mintzer, 1981). At least two contributions to γ are neglected in the present models: (1) mechanical strain associated with the effective small pore radius, and (2) coulombic repulsion associated with head groups lining the pore interior. Future versions that use a more realistic $\gamma(r)$ function should predict more larger pores. As further progress towards understanding electroporative molecular transport is achieved, the pore population will probably be found to operate somewhat like a sieve. If so, the distribution of pore sizes will be important. Again, it is clear that a description based on a single pore size is incomplete, because the average pore size usually changes significantly during electroporation.

Fractional aqueous area of the membrane

The transient aqueous pore model predicts that F_w is small for all reversible electroporation phenomena (Figs. 5, 9, and 13). Although dramatic reversible behavior occurs, $F_w(t)$ is found to be small, never exceeding 10^{-3}, i.e., about 0.1% of the membrane area. In contrast, for irreversible behavior (viz. rupture, a mechanical breakdown), $F_w(t) \rightarrow 1$ as the membrane is destroyed. The small maximum value of $F_w(t)$ emphasizes the idea that minor structural changes within the entire membrane can have significant consequences.

Change in the membrane capacitance

Clearly the membrane capacitance should also change, because aqueous pores have a significantly larger (factor of $K_w/K_m \approx 40$) capacitance per area than nonporated membrane. Thus, it is important to determine whether the transient pore population that is consistent with the dramatic reversible behavior of REB is also consistent with what is known experimentally about the change in capacitance. To our knowledge, there has been only one experimental determination of ΔC under electroporation conditions, for which the capacitance change associated with breakdown of an artificial planar bilayer membrane was found to be less than 2% (Chernomordik et al., 1982). The present theoretical model is in agreement, predicting $[\Delta C/C_0]_{max} \approx$ 1 to 2 $\times$ 10^{-2} during reversible electrical breakdown for the short square, exponential, and bipolar square pulses of Figs. 5, 9, and 13.

Although this approximate agreement for electroporation conditions is important, the transient aqueous pore model should be further tested by comparing (1) the predicted pore

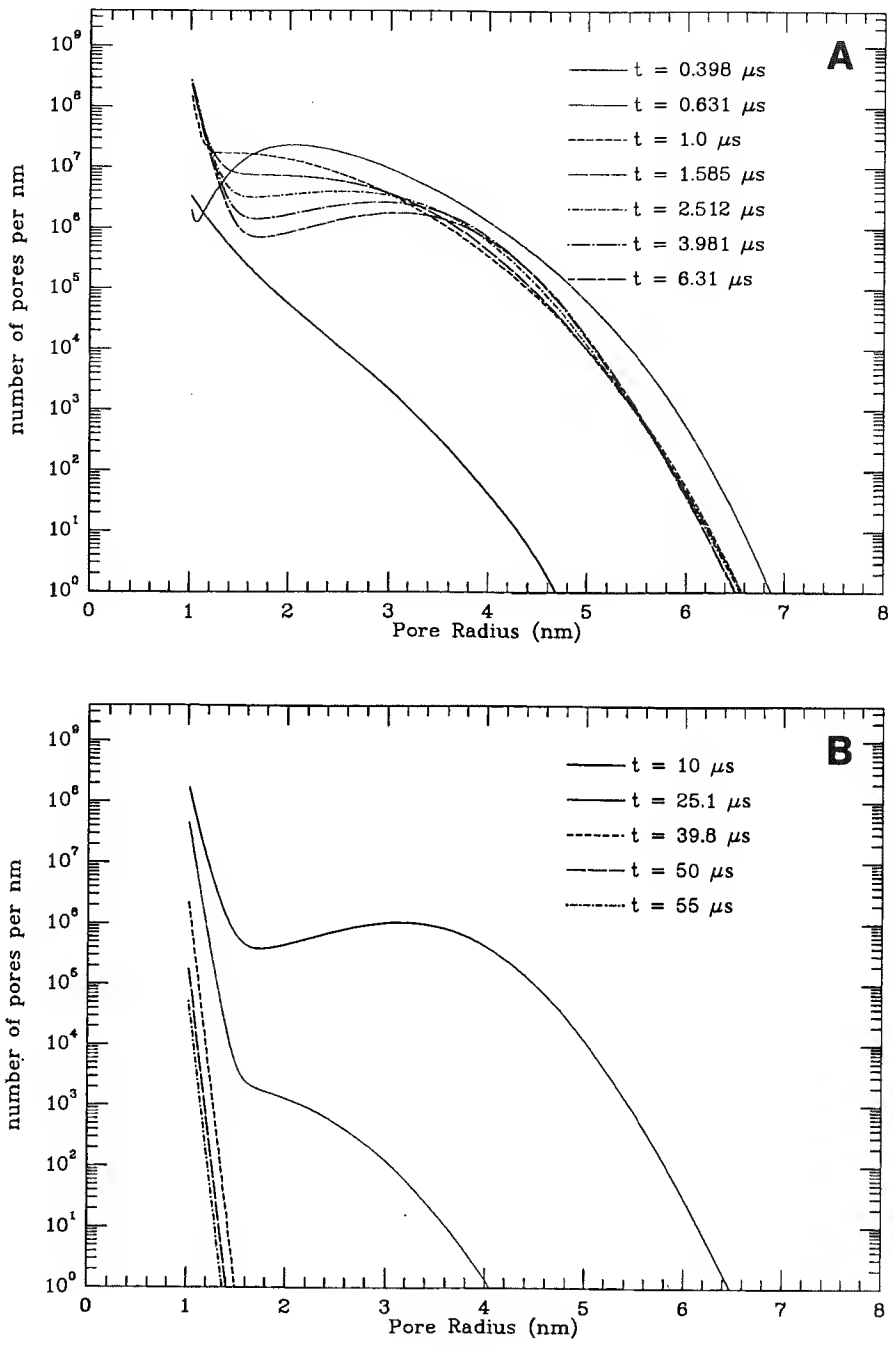

FIGURE 7 Pore population distributions at the indicated times, using the density function, $n(r,t)$ and Δr =0.026 nm as in Fig. 3. Note that the probability of having large, supracritical pores that cause rupture remains small. (*A*) $n(r, t)$ plots for t = 0.398–6.31 s. Note that the plots do not change significantly over the interval 0.631–6.31 μs. (*B*) For t = 10–55 μs.

contribution to $\Delta C/C_0$ with (2) the experimental measurements of $\Delta C/C_0$ at low transmembrane voltages that have been interpreted as being due to electrostriction of the entire membrane. At smaller voltages, electrostrictive thinning of the entire membrane has been suggested as the mechanism for capacitance change. For example, measurements by Alvarez and Latorre (1978) found that for U in the range $0 \leq U < 300$ mV, the capacitance of membranes formed from lipids depends on U according to $C(U) = C(0)[1 + \alpha_{AL}U^2]$. Here $C(0)$ is the membrane capacitance at zero transmembrane voltage, and $\alpha_{AL} \approx 0.02$ V^{-2} is the experimentally determined coefficient for "solvent free" bilayers believed to be representative of cell membranes. For $U \approx 0.3$ V, this gives $\Delta C/C_0 \approx 2 \times 10^{-3}$. More recently, measurements by Toyama et al. (1991) for a more compressible BLM revealed $\Delta C/C_0 \approx 10^{-2}$ at a smaller voltage (150 mV), and this was also attributed to electrostriction. Clearly the transient aqueous pore model is consistent with these results (Table 2), because it predicts a negligible contribution to $\Delta C/C_0$ in the low voltage regime.

Pore-pore separation and pore coalescence

We have also estimated the mean separation of pore centers, $\bar{S}_{pp}$. These computed results predict that if pores do not interact and, therefore, appear randomly, then pores are widely spaced in a planar membrane for essentially all electroporation phenomena (the exception is rupture, during which the

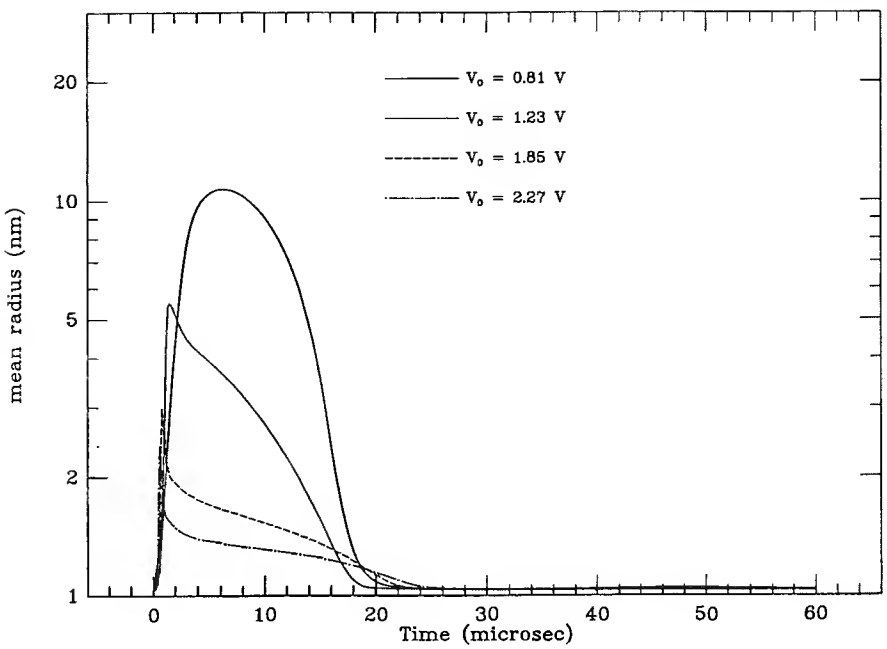

FIGURE 8 Mean radius, $\bar{r}(t)$, for the four exponential pulses of Fig. 6. Rupture has a low probability, as $\bar{r}$ remains small (cf. Figs. 2–4).

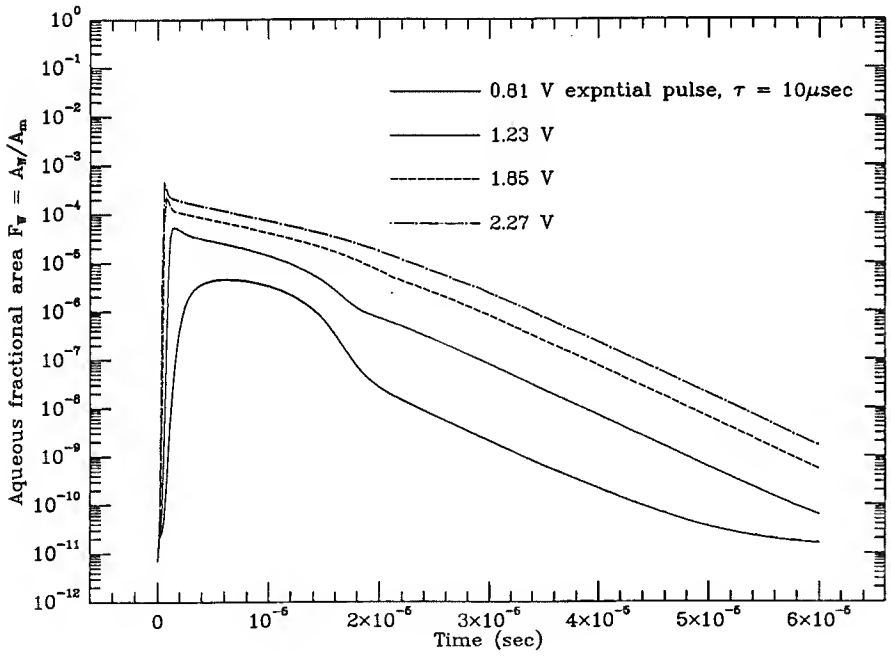

FIGURE 9 Aqueous fractional area, $F_w(t)$, for the exponential pulses of Fig. 6. Again $F_w(t) < 10^{-3}$, even when the largest number of pores occurs (REB).

membrane disappears as one or more pores expand to the membrane's boundary). For small pulses that cause insignificant electroporation, or for the larger pulses that result in a large number of pores, the mean spacing is less than about 30 mean pore diameters. This by itself would suggest that pore-pore encounter and subsequent coalescence is rare in flat membranes, in contrast to the suggested formation of "cracks" (Sugar et. al, 1987) by this mechanism.

Pore-pore "repulsion" and low probability of close occurrence

Interactions between pores could significantly alter the above prediction. One general type of expected interaction is through the perturbation of the transmembrane voltage by a conducting pore. A spatially inhomogeneous electric field is expected within the electrolyte near the entrances to a pore (Pastushenko and Chizmadzhev, 1982; Powell et al., 1986; Barnett and Weaver, 1991). For this reason, there is a nonzero component of the electric field parallel to the membrane surface, such that U increases away from a pore. Suppose a first pore exists. Then the probability of forming a second pore will be greatest at sites where U is largest, i.e., a site furthest from the first pore. This qualitative argument thus suggests that pore formation is not entirely random, and that pores will tend to form away from each other.

Moreover, in a flat membrane pores should migrate away from each other. The microscopic fluctuations that cause en-

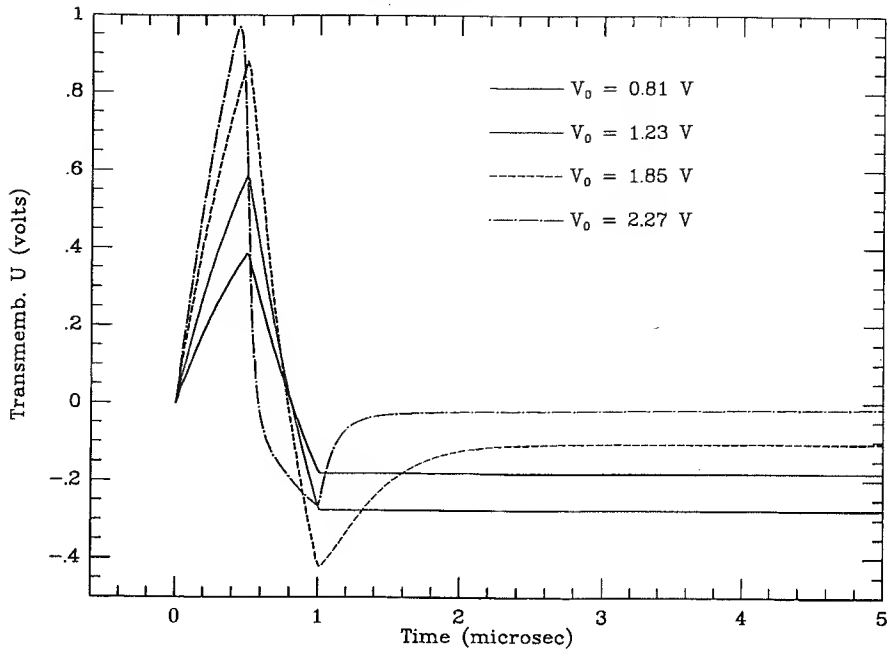

FIGURE 10 Transmembrane voltage, $U(t)$, for several symmetric bipolar square square pulses that first go positive, and then negative, with a width (time constant) of 1 μs. For the smaller pulses, the membrane acquires the less conductance, and results in more negatively charged valves at the end of the pulse. As the pulse amplitude is progressively increased, the membrane acquires a larger conductance, and is able to more completely discharge, so that the "final" value of U is progressively closer to zero.

try of high dielectric material (viz. water) into a membrane are larger in regions where U is larger. The "spreading resistance" perturbation of the electric field within the electrolyte due to a first pore results in a gradient in the tangential electric field at the site of a second pore. The contribution to U on the side furthest from the first pore is larger, so aqueous penetration fluctuations at the second pore's edge away from the first pore will be larger. As a result, the second pore will tend to grow more rapidly on the side away from the first pore and, by this mechanism, will migrate away from the first pore.

Real membranes, however, are not truly flat. Planar membranes are believed to support a variety of shape fluctuations, ranging from waves to indentations and dimples (Chizmadzhev et al., 1979; Bach and Miller, 1980; Lipowsky, 1991). More significantly, cell membranes are curved. In this case, the effect of the resulting tangential component of the electric field should be to cause migration of pores towards the region of larger U. Qualitatively, this could lead to pore-pore contact at the "polar caps" of a spherical cell; this appears to be the dominant mechanism by which pore contact could occur. As suggested previously, this could lead to pore coalescence (Sugar et al., 1987).

Negligible pore-pore magnetic interaction

The magnetic attraction due to current flow through nearly parallel pores will cause a weak attraction. The order of magnitude of this interaction can be estimated by considering two parallel current filaments that correspond to maximum pore currents. The minimum resistance of a small pore is $R_p \approx \rho_{bulk} h/\pi r_{min}^2 \approx$ (0.7 ohm m) (2.8 $\times$ 10^{-9} m)/(π) (1 $\times$ 10^{-9} m)^2 $\approx$ 10^9 ohm. A typical large transmembrane voltage is of order 1 V, so the maximum pore current is of order 10^{-9} A. The attractive magnetic force, therefore, is of order $F_{magnetic} \approx \mu_0 I_{pore}^2 h/2\pi S_{pp,min} \approx$ ($4\pi \times 10^7$ henry m^{-1}) (10^{-9} A)^2(2.8 $\times$ 10^{-9} m)/(2π) (2 $\times$ 10^{-9} m) $\approx$ 3 $\times$ 10^{-25} N. The work done to move one pore a minimal characteristic distance of $S_{pp,min} = 2r_{min}$ is used to estimate the associated change in energy, $\Delta W_{magnetic} \approx 2r_{min} F_{magnetic} \approx$ (2)(10^{-9} m) (3 $\times$ 10^{-25} N) = 6 $\times$ 10^{-34} J $\approx$ 10^{-13} kT. where kT = 4 $\times$ 10^{-21} J is the thermal energy at 37°C. This order of magnitude estimate shows that the magnetic interaction is negligible, even if 100-fold larger pores with 10^4 greater currents (neglecting the spreading resistance) were considered.

SUMMARY

We have estimated properties and behavior of the pore populations that are consistent with the electrical and mechanical behavior due to electroporation in planar bilayer membranes. Except for the irreversible case of rupture at moderate U, only a small fraction (<10^{-3}) of the membrane area becomes occupied by aqueous pores. Consistent with this, a rapid but very small change in membrane capacitance is estimated to occur for reversible electroporation. This agrees with experimental evidence and provides justification for the approximation that C is constant in transient aqueous pore theories, here entering through Eq. 6. Finally, because relatively few pores are predicted to appear, the mean pore spacing is large, reaching a minimum of about 60 nm (about 30 minimum pore diameters). Moreover, a qualitative argument that considers the electric field component parallel to the membrane due to a conducting pore suggests that pores are most likely to form away from existing pores, and then to migrate apart. Magnetic attraction of pores is found to be negligible. Together this suggests that flat membranes rarely have pores close together and that pore coalescence in this case is unlikely. However, the opposite is predicted (qualitatively) for

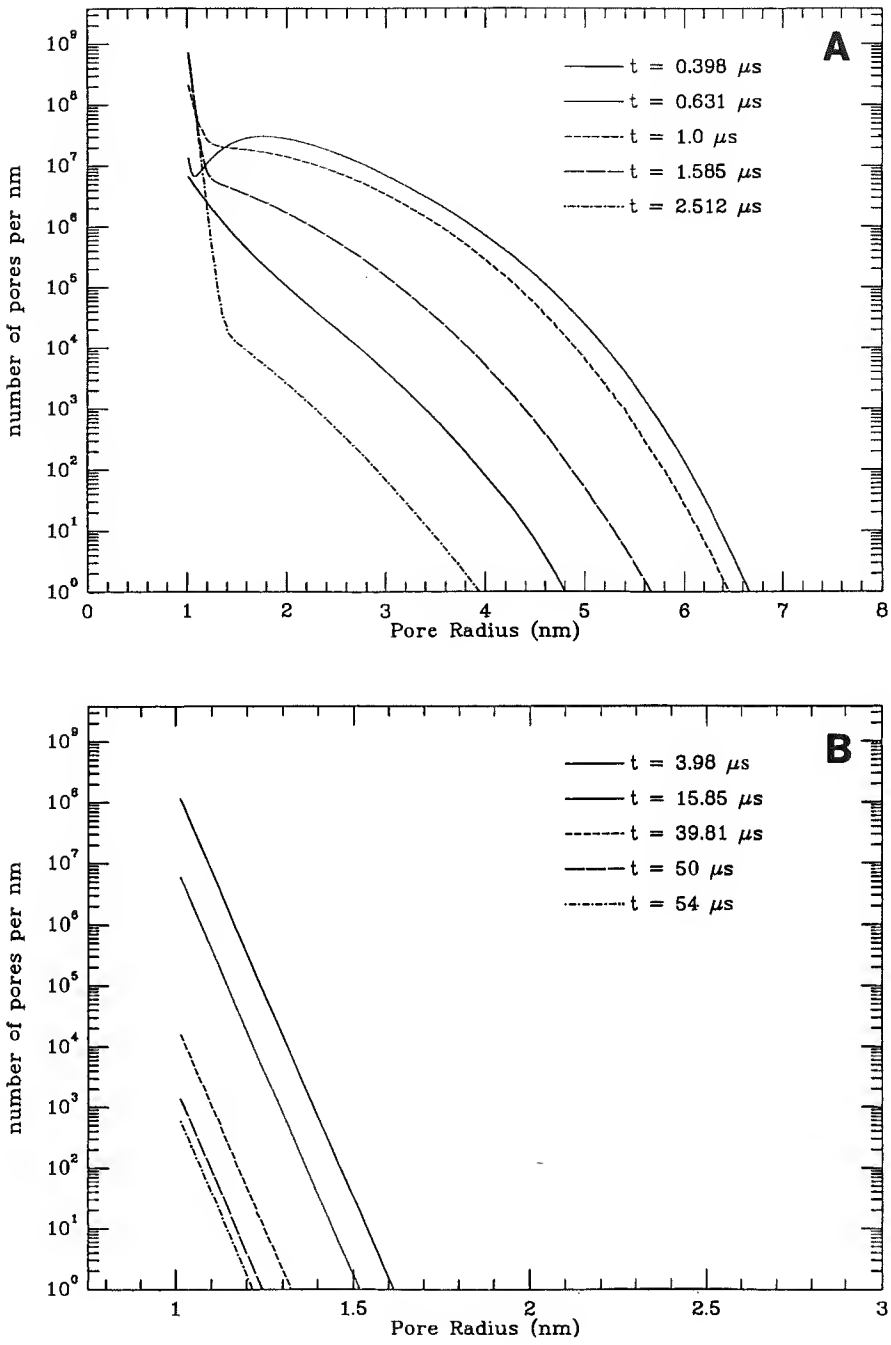

FIGURE 11 Pore population distributions for the case of the bipolar square square pulses. Note that no rupture is predicted. In the present version of the theory, the pore-expanding pressure due to the elevated U is a function of U^2, so the pore population is enlarged during both the positive and negative portions of the pulse. (*A*) $n(r,t)$ plots for t = 0.398–2.52 μs. Note that the population rapidly expands, and has begun collapse (recovery) at t = 1.0 μs. (*B*) For t = 3.98–54 μs.

the curved membranes of cells, for which pores are expected to migrate to the regions with the greatest transmembrane voltage, so that pore coalescence may then occur. For all of the predicted electroporation behavior, it was found that a single pore size does not allow essential aspects of electroporation to be described, because even the average pore size changes significantly. This emphasizes the need to consider explicitly a dynamic, heterogeneous pore population as an integral part of electroporation.

We thank T. E. Vaughan, S. Dyer, V. G. Bose, and A. Barnett for assistance and stimulating discussions.

This work supported partially by Army Research Office Grant No. DAAL03-90-G-0218, National Institutes of Health Grant ES06010, and a computer equipment grant from Stadwerke Düsseldorf, Düsseldorf, Germany.

APPENDIX: ORIGIN OF SOME PARAMETERS

The motivation for some of the model's parameters has not been fully provided in our previous papers. For this reason, we briefly describe the reasoning that led to our currently used values of "a" (coefficient of U^2 in the voltage-dependent component of the barrier to pore creation), δ_c (voltage-independent component of the barrier to pore creation), δ_d (voltage-independent component of the barrer to pore destruction),

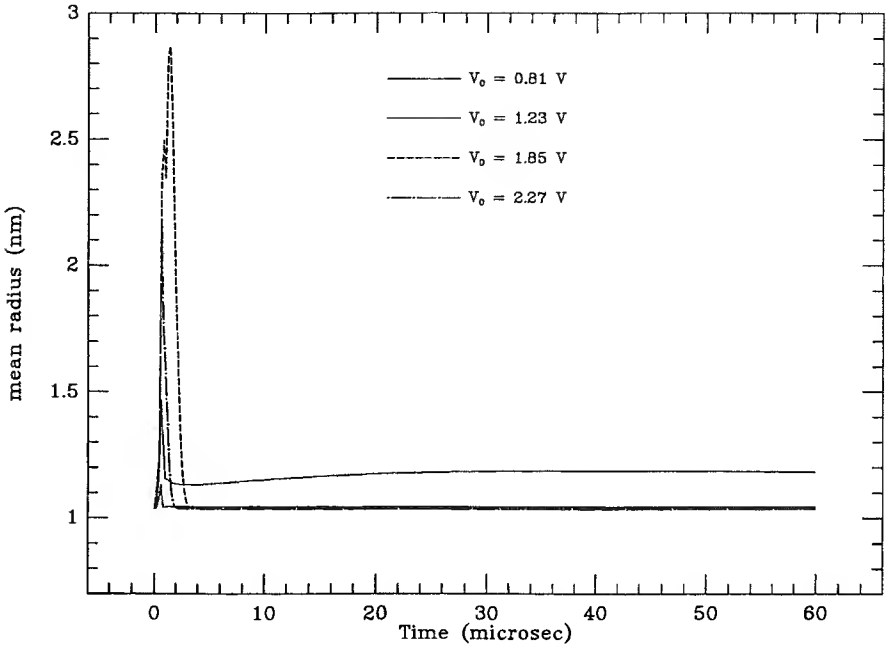

FIGURE 12 Mean pore radius, $\bar{r}(t)$, for the bipolar square pulses.

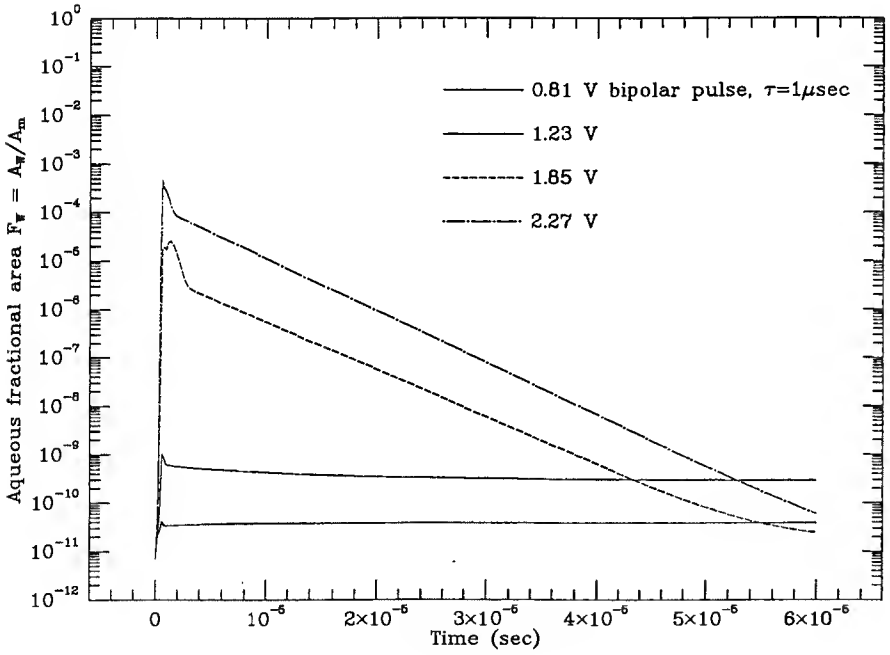

FIGURE 13 Aqueous fractional area, $F_w(t)$ for the bipolar square pulses. Again $F_w(t)$ remains less than 10^{-3}.

$\nu_0 = \nu/V_m = \nu/A_m h$ (ν_0 is the attempt rate density, and ν is the corresponding prefactor of the Boltzmann factor containing δ_c), χ (prefactor of Boltzmann factor containing δ_d), and D_p (diffusion constant in pore radius space). It is emphasized that although the simulation exhibits several key features of electroporation (simple membrane charging, rupture, incomplete REB, and then REB as the pulse magnitude is increased), it is not entirely accurate. Furthermore, as noted previously (Barnett and Weaver, 1991), given the multiparametric nature of the model and the relative lack of quantitative experimental data available, it is not presently realistic to seek parameter values by numerical fits. With these limitations in mind, the introduction of these particular parameters, and the selection of their numerical values, should be regarded as approximate and illustrative, rather than definitive.

A starting point for obtaining these parameters considers the steady state at zero transmembrane voltage. Specifically, we assume that an artificial planar bilayer membrane at $U = 0$ has a time average number of pores, $\bar{N}$, which is small. The actual number is not known, so a plausibly small value, of order 10, was chosen. We did not want $\bar{N} \leq 1$, because experience in working with the highly nonlinear simulation had shown us that key electroporation-related phenomena would not then readily occur. Our approach was to consider the steady state at $U = 0$, and to then find values of δ_c, δ_d, χ, and ν_0 that were individually plausible, and that also allowed the model to exhibit basic electroporation behavior when used with a range of short voltage pulses. A lengthy series of simulation trials with short square pulses was then used to guide further the choice of all the parameter values.

TABLE 2 Illustrative Fractional Capacitance Changes

Pulse type	$[\Delta C \div C_0]_{max}$	Phenomenon
2.27 V, 0.4 μs square	1×10^{-2}	Reversible discharge to zero (Fig. 2)
2.27 V, 10 μs exponential	2×10^{-2}	Reversible discharge to zero (Fig. 6)
2.27 V, 1 μs bipolar square	2×10^{-2}	Reversible discharge to zero (Fig. 10)
0.35 V, 50 μs square	1×10^{-5}	Steady 0.35 V achieved*
0.20 V, 50 μs square	2×10^{-9}	Steady 0.20 V achieved*

* Conditions of negligible electroporation, i.e., creation of only a few pores and, therefore, insignificant pore-related conduction to provide discharge of the membrane on a rapid time scale. Under these conditions, the main contribution to ΔC is believed to be electrostriction (Alvarez and Latorre, 1978; Toyama et al., 1991). These predicted steady values of $[\Delta C/C_0]$ due to pores were computed by using a 50 μs square pulse in the simulation, which resulted in the membrane achieving $U = 0.35$ and 0.20 V, respectively. Note that 50 μs is considerably longer than needed to achieve a steady state (see Fig. 2 for the 0.81-V pulse). The significance of these two smaller, 50-μs pulses is that the transient aqueous pore model predicts achievement of steady changes that are significantly smaller than the experimental observations in this range. For example, Alvarez and Latorre found $[\Delta C/C_0] \approx 2 \times 10^{-4}$ at $U \approx \pm 0.1$ V (Alvarez and Latorre, 1978), and Toyama et al. (1991) found $[\Delta C/C_0] \approx 2 \times 10^{-3}$ to 10^{-2} at $U \approx \pm 0.15$ V. In the low voltage region, these experimental values are much larger than the predicted pore contribution, which demonstrates that the pore model does not violate experimental observations in the low voltage, nonelectroporation region.

The steady-state probability density function, $n(r)$, is obtained by setting the left side of Eq. 5 equal to zero. A solution of the resulting ordinary differential equation is

$$n(r) = n_0 e^{-\Delta E/kT}, \tag{A1}$$

This function is a Boltzmann factor multiplied by a normalization constant, and it describes the distribution of pore sizes for any constant transmembrane voltage (Weaver et al., 1984). It is like a "law of atmospheres," in that the probability of finding an entity (here a pore) decreases exponentially as the entity energy increases, with only thermal fluctuations available to populate the system.

We next use the $U = 0$ case to aid in selection of the basic parameters that govern pore creation and destruction. At $U = 0$ the contribution of the membrane surface energy, Γ, is small compared to that of the edge energy, γ. This is a consequence of the "barrier" (maximum value of $\Delta E(r, U = 0)$) being large, so that the probability of having a large pore is extremely small, and is consistent with the interpretation that rupture at $U = 0$ is negligible. In this case only the first term in Eq. 1 is significant, and ΔE can be linearized to $\Delta E \approx 2\pi\gamma r$. This means that

$$n(r) \approx n_0 e^{-2\pi\gamma r/kT} = n_0 e^{-r/\lambda_r}, \tag{A2}$$

where $\lambda_r = kT/2\pi\gamma \approx 3 \times 10^{-11}$ m is a characteristic length in pore radius space. The small size of λ_r means that at zero transmembrane voltage the pore population falls off extremely rapidly with increasing r. Therefore, all of the pores at $U = 0$ have $r \approx r_{min}$. This, in turn, justifies our approximating Eq. 1 by only the first term.

We can now find an expression for the number of time average pores, $\tilde{N}$, in a particular planar membrane by integrating $n(r)$ from r_{min} to ∞.

$$\tilde{N} = \int_{r_{min}}^{\infty} n_0 e^{-r/\lambda_r}\, dr = n_0 \lambda_r e^{-r_{min}/\lambda_r} \tag{A3}$$

To proceed, n_0 must be determined. Clearly the average number of pores present is determined by a balance between pore creation and destruction. Eq. 4, which describes pore destruction, involves the factor

$$n(r_{min}) = n_0 e^{-r_{min}/\lambda_r}. \tag{A4}$$

The steady-state condition of balance of creation and destruction is simply $(\dot{N})_c = (\dot{N})_d$, which at $U = 0$ becomes

$$\nu e^{-\delta_c/kT} = \chi n(r_{min}) e^{-\delta_d/kT} = \chi n_0 e^{-r_{min}/\lambda_r} e^{-\delta_d/kT}. \tag{A5}$$

As shown in the main part of this paper, for reversible electroporation involving many pores at large U, the pores are always widely spaced. At $U = 0$ the few pores present are essentially independent. Thus, if we think of the pore creation and destruction as being governed by a transition from a "zero pore state" for the entire membrane to a "one pore state," we expect that the barrier for a "0 → 1" transition (δ_c) will be larger than the barrier for a "1→0" transition (δ_d). It is generally believed that pore creation proceeds by first forming hydrophobic pores, followed by surmounting a large barrier to create a minimum size hydrophilic pore (Abidor et al., 1979). In fact, at $U = 0$ both δ_c and δ_d are believed to be large compared to their difference, $\delta_c - \delta_d$. For simplicity, therefore, we have assumed that that the same barrier height governs both the "0 → 1" and "1→0" transitions, and we have accounted for the difference in barrier heights through their very different prefactors ν and χ (see below). That is, for convenience we have assumed that $\delta_c = \delta_d$, and we have incorporated the rate difference into the values of the corresponding barrier prefactors, ν and χ. With this simplification, Eq. A5 becomes

$$\nu = \chi n_0 e^{-r_{min}/kT}. \tag{A6}$$

We next consider the relationship between ν and χ. The relative magnitudes of ν and χ can be estimated by arguing: (1) that creation of a pore can occur essentially anywhere in the membrane, because only a small fraction of the membrane area is occupied by pores, and (2) the destruction of a pore is a highly localized event. This means that creation events can involve fluctuations within the entire volume of the membrane, whereas destruction events must be localized to a much smaller volume, one that is typical of the membrane molecules associated with a pore of radius r_{min}. More specifically, we argue that the order of magnitude ratio is

$$\frac{\chi}{\nu} \approx \frac{2\pi r_{min}(\delta r)h}{A_m h} \approx \frac{2\pi r_{min}^2}{A_m} \approx 5 \times 10^{-12}, \tag{A7}$$

where $(\delta r) \approx r_{min}$ is an estimator of the radial extent of an annular volume having fluctuations that can destroy a pore. The significant inequality implied by Eq. A7 also suggests that minimum size pores will require much longer times for their destruction than fo their creation, i.e., that pores may have relatively long lifetimes. This is consistent with the observations of Chizmadzhev and co-workers, who find that pores, which are believed to be near the minimum size, have lifetimes of many seconds (Abidor et al., 1979).

We now find $\tilde{N}$ by recognizing that the steady state is independent of kinetics, because only the ratio ν/χ is important, and we write n_0 as

$$n_0 = \left[\frac{\nu}{\chi}\right] e^{+r_{min}/kT} \approx 1.2 \times 10^{24}\ \mathrm{m}^{-1}. \tag{A8}$$

Substitution into Eq. A2 yields $\tilde{N} \approx 7$, which is consistent with the assumed constraint that fewer than 10 pores should be present at $U = 0$. This result can also be obtained using the exact expression given in Eq. 28 in Barnett and Weaver (1991).

A major goal of the simulation is to describe dynamic behavior, and this is significantly more difficult than treating the steady state. Given our assumptions and approximations, there remain three undetermined parameters that directly enter into the description of pore creation and destruction. There is (1) a single voltage-independent barrier ($\delta_c = \delta_d$), (2) a voltage-dependent barrier component for pore creation (aU^2 in $\Lambda = \delta_c - aU^2$), and (3) one prefactor (ν), because the ratio ν/χ is fixed by Eq. A7. A fourth parameter, D_p, the diffusion constant in pore radius space, only indirectly affects pore creation and destruction.

With this in mind, we next consider the parameter "a" in aU^2. Equation 3 describes the pore creation rate, $(\dot{N})_c$, in terms of a Boltzmann factor and an attempt rate (prefactor). The energy barrier of the Boltzmann factor, $\Lambda = \delta_c - aU^2$, contains both a voltage-independent component and a voltage-dependent component. The total barrier to pore creation, $\Lambda = \delta_c - aU^2$, is expected to be much larger than the pore energy for a minimum size pore ($r = r_{min}$). For simplicity we assumed the form $\Lambda = \delta_c - aU^2$ and used the constraint $\Lambda > \Delta E(r_{min}, U)$. The origin of the value $\delta_c = 2 \times 10^{-19}$ J was mentioned above. We then used an order of magnitude estimate for "a" by considering the order of magnitude of the energy aU^2 for a pore size intermediate to the minimum hydrophilic pore size ($r_{min} = 1$ nm) and the hydrophobic pores (radii of zero up to r_{min}; Abidor et al., 1979). Specifically, we used $r_{intermediate} = 0.16$ nm, which corresponds to the value

$$a = \frac{\epsilon_0(K_w - K_l)\pi r^2_{intermediate}}{h} \approx 1.9 \times 10^{-20}\ \text{F}, \qquad \text{(A9)}$$

which is a capacitance associated with this size hypothetical intermediate (transitional state) hydrophobic pore.

Once created, however, pores also expand and contract according to Eq. 5, for which the relevant parameter is D_p and which, through the Einstein relation, can also be considered as a mobility in radius space (Powell and Weaver, 1986). The remaining three parameters were obtained by considering both order of magnitude estimates of possible magnitudes, and by carrying out many simulations of electroporation dynamics. First we consider δ_c in the context of Eq. 3. The minimum energy to make a pore of radius r_{min} is $\Delta E(r_{min}, U)$. Inspection of Eq. 1 shows that the voltage-independent component of ΔE is the minimum possible value for δ_c, viz.

$$(\delta_c)_{min} = 2\pi\gamma r_{min} - \pi\Gamma r^2_{min} = 1.2 \times 10^{-19}\ \text{J} = 30\ kT. \qquad \text{(A10)}$$

However δ_c must be larger than this value, because $(\delta_c)_{min}$ does not take into account the the assumed transition of a hydrophobic pore to a hydrophilic pore, which is unknown but believed to be significant (Abidor et al., 1979; Glaser et al., 1988). Therefore, somewhat arbitrarily but also using simulation trial results, the value $\delta_c = 2 \times 10^{-19}$ J = 50 kT was chosen.

The attempt rate density was originally estimated by considering only the molecules of a fluid membrane and treating these molecules as a dense ideal gas. This gave an order of magnitude estimate, $\nu_0 \approx 2 \times 10^{38}\ \text{s}^{-1}\ \text{m}^{-3}$ (Weaver and Mintzer, 1981). Subsequently, it was recognized that ν_0 could be expressed in terms of other model parameters (Powell and Weaver, 1986), which led to another estimate, $\nu_0 \approx 5 \times 10^{32}\ \text{s}^{-1}\ \text{m}^{-3}$. As noted there, the large (almost six orders of magnitude) difference is not actually significant, because it multiplies a Boltzmann factor. In the present paper we carried out lengthy exploration of the simulation for many square pulse magnitudes, and in the process we found that the presently used value $\nu_0 = \nu/A_{mh} \approx 2 \times 10^{42}\ \text{s}^{-1}\ \text{m}^{-3}$ resulted in successful simulation of electroporation behavior. However, a rigorous basis for ν_0 is still lacking.

The remaining parameter whose value needs explanation is the currently used value $D_p = 5 \times 10^{-14}\ \text{m}^2\ \text{s}^{-1}$. The diffusion constant in pore radius space was originally introduced for electroporation by Chizmadzhev and his coworkers in their 1979 series of papers (Abidor et al., 1979). In one of our earlier papers (Powell and Weaver, 1986), an order of magnitude estimate of the magnitude was made by treating liquid water as a dense ideal gas, but there was no attempt to include the effect of water's viscosity. This gave the value $D_p = 1.1 \times 10^{-12}\ \text{m}^2\ \text{s}^{-1}$. However, the effect of viscosity should be to slow transport processes and, therefore, to yield a smaller value. In the current version of the model (Barnett and Weaver, 1991), a 20-fold smaller value of $D_p = 5 \times 10^{-14}\ \text{m}^2\ \text{s}^{-1}$ was used, again based partly on many simulation results.

In summary, the introduction of the particular parameters, and the selection of their numerical values, is based on plausible physical constraints and on the results of many simulation trials. The parameters that can be obtained using steady-state behavior are generally better understood than those that are intimately involved in the dynamic behavior. In all cases, it is important to recognize that relatively little quantitative information is available regarding detailed electroporation behavior and, therefore, that the simulation should be regarded as approximate and illustrative, not definitive. We believe that although it is significant that the simulation can describe quantitatively some essential features of electroporation, much more remains to be done.

REFERENCES

Abidor, I. G., V. B. Arakelyan, L. V. Chernomordik, Yu. A. Chizmadzhev, V. F. Pastushenko, and M. R. Tarasevich. 1979. Electric breakdown of bilayer membranes. I. The main experimental facts, and their qualitative discussion. *Bioelectrochem. Bioenerg.* 6:37–52.

Alvarez, O., and R. Latorre. 1978. Voltage-dependent capacitance in lipid bilayers made from monolayers. *Biophys. J.* 21:1–17.

Bach, D., and I. R. Miller. 1980. Glyceryl monooleate black lipid membranes obtained from squalene solutions. *Biophys. J.* 29:183–188.

Barnett, A., and J. C. Weaver. 1991. Electroporation: a unified, quantitative theory of reversible electrical breakdown, and rupture. *Bioelectrochem. Bioenerg.* 25:163–182.

Benz, R., F. Beckers, and U. Zimmermann. 1979. Reversible electrical breakdown of lipid bilayer membranes: a charge-pulse relaxation study. *J. Membr. Biol.* 48:181–204.

Blank, M., editor. 1993. Electricity and Magnetism in Biology and Medicine. San Francisco Press, San Francisco.

Chang, D. C., B. M. Chassy, J. A. Saunders, and A. E. Sowers, editors. 1992. Guide to Electroporation and Electrofusion. Academic Press, New York.

Chernomordik, L. V., S. I. Sukharev, I. G. Abidor, and Yu. A. Chizmadzhev. 1982. The study of the BLM reversible electrical breakdown mechanism in the presence of UO_2^{2+}. *Bioelectrochem. Bioenerg.* 9:149–155.

Chizmadzhev, Yu. A., V. B. Arakelyan, and V. F. Pastushenko. 1979. Electric breakdown of bilayer membranes. III. Analysis of possible mechanisms of defect origin. *Bioelectrochem. Bioenerg.* 6:63–70.

Glaser, R. W., S. L. Leikin, L. V. Chernomordik, V. F. Pastushenko, and A. I. Sokirko. 1988. Reversible electrical breakdown of lipid bilayers: formation, and evolution of pores. *Biochim. Biophys. Acta.* 940: 275–287.

Hibino, M., M. Shigemori, H. Itoh, K. Nagyama, and K. Kinosita. 1991. Membrane conductance of an electroporated cell analyzed by submicrosecond imaging of transmembrane potential. *Biophys. J.* 59:209–220.

Lipowsky, R. 1991. The conformation of membranes. *Nature.* 349:475–481.

Neumann, E., A. Sowers, and C. Jordan, editors. 1989. Electroporation and Electrofusion in Cell Biology. Plenum Press, New York.

Orlowski, S., and L. M. Mir. 1993. Cell electropermeabilization: a new tool for biochemical and pharmacological studies. *Biochim. Biophys. Acta.* 1154:51–63.

Pastushenko, V. F., and Yu. A. Chizmadzhev. 1982. Stabilization of conducting pores in BLM by electric current. *Gen. Physiol. Biophys.* 1:43–52.

Powell, K. T., E. G. Derrick, and J. C. Weaver. 1986. A quantitative theory of reversible electrical breakdown. *Bioelectrochem. Bioelectroenerg.* 15: 243–255.

Powell, K. T., and J. C. Weaver. 1986. Transient aqueous pores in bilayer membranes: a statistical theory. *Bioelectrochem. Bioelectroenerg.* 15: 211–227.

Sugar, I. P. 1981. The effects of external fields on the structure of lipid bilayers. *J. Physiol. (Paris).* 77:1035–1042.

Sugar, I. P., and E. Neumann. 1984. Stochastic model for electric field-induced membrane pores: electroporation. *Biophys. Chemistry.* 19: 211–225.

Sugar, I. P., W. Förster, and E. Neumann. 1987. Model of cell electrofusion: membrane electroporation, pore coalescence, and percolation. *Biophys. Chem.* 26:321–335.

Toner, M., and E. G. Cravalho. 1990. Kinetics and likelihood of membrane rupture during electroporation. *Phys. Lett.* 143:409–412.

Toyama, S., A. Nakamura, and F. Toda. 1991. Measurement of voltage dependence of capacitance of planar bilayer lipid membrane with a patch clamp amplifier. *Biophys. J.* 59:939–944.

Tsong, T. Y. 1991. Electroporation of cell membranes. *Biophys. J.* 60: 297–306.

Weaver, J. C. 1993a. Electroporation: a general phenomenon for manipulating cells and tissue. *J. Cell. Biochem.* 51:426–435.

Weaver, J. C. 1993b. Electroporation: a Dramatic, non-thermal electric field phenomenon. *In* Electricity and Magnetism in Biology and Medicine. M. Blank, editor. 95–100.

Weaver, J. C., and A. Barnett. 1992. Progress towards a theoretical model of electroporation mechanism: membrane electrical behavior and molecular transport. *In* Guide to Electroporation and Electrofusion. D. C. Chang, B. M. Chassy, J. A. Saunders, and A. E. Sowers, editors. Academic Press, New York. 91–117.

Weaver, J. C., and R. A. Mintzer. 1981. Decreased bilayer stability due to transmembrane potentials. *Phys. Lett.* 88:57–59.

Weaver, J. C., K. T. Powell, R. A. Mintzer, H. Ling, and S. R. Sloan. 1984. The electrical capacitance of bilayer membranes: the contribution of transient aqueous pores. *Bioelectrochem. Bioelectroenerg.* 12: 393–404.